Multimedia Tools and Applications (2024) 83:7681–7719
https://doi.org/10.1007/s11042-023-15812-0

SCGJO: A hybrid golden jackal optimization with a sine cosine algorithm for tackling multilevel thresholding image segmentation

Jinzhong Zhang[1] · Gang Zhang[1] · Min Kong[1] · Tan Zhang[1]

Received: 4 August 2022 / Revised: 28 April 2023 / Accepted: 10 May 2023 /
Published online: 10 June 2023

Abstract
Multilevel thresholding is a fundamental, substantial and constructive technique that has been widely recognized and concerned in recent years. However, the computational complexity rises as the threshold level raises. The golden jackal optimization (GJO) imitates discovering prey, tracking and encircling prey, and trapping prey by employing a collaborative foraging mechanism. To eliminate the GJO's drawbacks, such as premature convergence, inferior computation accuracy and sluggish convergence rate, this paper proposes a hybrid golden jackal optimization with a sine cosine algorithm (SCGJO) based on Kapur's entropy to tackle the multilevel thresholding image segmentation, the intention is to actualize the accurate threshold values and the maximal fitness values. The SCGJO not only has fantastic adaptability and reliability to promote the complementary benefits and boost the convergence accuracy but also integrates exploration and exploitation to mitigate search stagnation and arrive at the ideal value. The experimental results demonstrate that the SCGJO is superior to the other algorithms and has a quicker convergence rate, higher computation accuracy, greater segmentation quality and stronger stability. In addition, the SCGJO is a steady and trustworthy approach for tackling image segmentation.

Keywords Multilevel thresholding · Golden jackal optimization · Sine cosine algorithm · Kapur's entropy · Image segmentation

1 Introduction

The image segmentation is a momentous prerequisite for the image process, image analysis and image comprehension. The adaptability and correctness of image segmentation influence the object extraction, detection and recognition and the effectiveness of follow-up work to a certain extent, and the primary aim is to separate an assigned image into several distinct and consistent sections that have the best similarity and features in terms of the grayscale, texture, color, pattern, histogram, edge and geometric

✉ Gang Zhang
zhanggang@wxc.edu.cn

[1] School of Electrical and Optoelectronic Engineering, West Anhui University, Lu'an 237012, China

shape, and then to retrieve the constructive sections [2, 11, 16, 21, 34]. The research problem and the image segmentation's quality are strongly associated, and greater segmentation quality signifies that the algorithm has a higher segmentation precision and efficiency. Threshold segmentation has certain advantages, such as low computational cost, simple implementation, fast operation speed, high segmentation precision, strong robustness and stability. The hybrid evolutionary algorithm with threshold segmentation method is utilized to promote optimization effectiveness and segmentation quality, such as the bat algorithm (BA) [44], dingo optimization algorithm (DOA) [7], flower pollination algorithm (FPA) [43], moth flame optimization (MFO) [26] and sine cosine algorithm (SCA) [27].

Ma et al. combined an upgraded whale optimization approach the Otsu to address the image segmentation, this algorithm maintained strong stability and excellent segmentation quality [25]. Liu et al. established an integrated remote optimization approach to address image segmentation, this algorithm exhibited significant stability and resilience to maintain better convergence accuracy and segmentation quality [23]. Agrawal et al. employed an adaptive whale optimization approach to address the color image segmentation, this algorithm combined exploration with exploitation to determine better segmentation results [4]. Wu et al. designed a modified sparrow search method to address image segmentation, this algorithm retained tremendous adaptability and global search to mitigate premature convergence [41]. Sharma et al. cultivated an updated firefly algorithm to address image segmentation, this algorithm identified a significant exploration to discover the most suitable solution [31]. Mookian et al. generated an upgraded sine cosine algorithm to address the image segmentation, this algorithm exhibited stronger calculation precision and superior segmentation accuracy [28]. Li et al. adopted a harmony search algorithm to address the image segmentation, this algorithm was both productive and workable to determine a quicker convergence accuracy and greater segmentation quality [22]. Patra et al. studied on moth flame method and whale optimization method for image segmentation, these algorithms have a substantial optimization ability to determine the overall best value [30]. Gill et al. suggested a teacher-learner based optimization to address the image segmentation, the feasibility and practicality of this algorithm have been proven [15]. Vijh et al. developed a hybrid bio-inspired algorithm with an artificial neural network to address image segmentation, this algorithm altered both the global ability and the local ability to determine a superior segmentation effect [37]. Si et al. designed the chimp optimization method to segment the medical image, this algorithm exhibited excellent stability and resilience to maximize the segmentation accuracy and optimization efficiency [33]. Subasree et al. established a multi-objective emperor penguin approach to address the image segmentation, this algorithm attained remarkable reliability and stability to discover the best threshold values [35]. Naik et al. designed an adaptive opposition slime mold algorithm to address medical image segmentation, this algorithm produced significant stability and robustness to identify the best value [29]. Das et al. devised an opposition equilibrium optimization based on the error minimization strategy to address image segmentation, this algorithm exhibited extensive exploration and exploitation to acquire the segmentation quality [12]. Liu et al. created an adaptive region-growing approach to address image segmentation, this algorithm had significant adaptability and stability to accomplish the best segmentation effect [24]. Zhang et al. combined a coupled chaotic system with the Otsu threshold method for medical image segmentation, this algorithm had excellent robustness and the better segmentation effect [45]. Wang et al. submitted an adaptive firefly algorithm to address the image segmentation, this algorithm had better segmentation quality,

optimization accuracy and computation time [38]. Houssein et al. designed an expanded chimp optimization method to address medical image segmentation, this algorithm boosted the convergence efficiency and calculation precision to attain the best solution [17]. Al-Rahlawee et al. adopted the black widow optimization based on the Otsu to address the image segmentation, this algorithm showed tremendous exploitation to supply superior results [5]. Anitha et al. clarified a modified whale optimization approach to address the color image segmentation, this algorithm obtained the best segmentation effect and the overall best value [6]. Duan et al. submitted a modified cuckoo search approach with the Otsu to address the image segmentation, this algorithm had sufficient optimization efficiency to determine the best fitness value [14]. Jiang et al. created an upgraded teaching-learning-based optimization method to address image segmentation, this algorithm had fantastic effectiveness and feasibility [19]. Houssein et al. utilized an upgraded marine predators algorithm to address the image segmentation, this algorithm had a significant exploration and exploitation to determine the better segmentation quality [18]. Abdel-Basset et al. combined a whale optimization approach with a unique technique to address color image segmentation, this algorithm had superiority and reliability to arrive at the best segmentation results [3]. Dinkar et al. introduced an equilibrium optimization approach based on Laplace distribution and opposition-based learning mechanism to address the image segmentation, this algorithm was verified to be superior to other appraoches [13]. Yan et al. highlighted a altered water wave optimization to address the image segmentation, this algorithm had excellent robustness and exploration to determine the better convergence accuracy and segmentation quality [42]. Chen et al. integrated the particle swarm optimization with sine cosine acceleration coefficients to address the numerical optimization issues, this algorithm had sufficient predictability and reliability to attain the better convergence accuracy [9]. Varga proposed visual saliency to address the image quality assessment, this method had great stability and robustness to determine the better results [36]. Shi et al. utilized three features fusion to design a trustworthy reference color image quality assessment and assess the image distortion, this method had a significant stability and search ability to determine the high accuracy [32].

The GJO, inspired by the jackals' collaborative foraging behavior, mimics discovering prey, tracking and encircling prey, and trapping prey to discover the global optimal value [10]. To overcome premature convergence, inferior computation accuracy and sluggish convergence rate of the basic GJO, the SCA is introduced. The SCGJO based on Kapur's entropy is presented to address the image segmentation, the intention is to actualize the accurate threshold value and the maximum fitness value. The SCGJO not only executes extensive exploration and exploitation to mitigate search stagnation and determine the ideal value but also achieves complementary benefits to promote convergence accuracy and segmentation quality. A series of experiments are employed to demonstrate the stability and resilience of the SCGJO, the segmentation results are contrasted with those of BA, DOA, FPA, MFO, SCA, and GJO by achieving the maximum Kapur's entropy. The various evaluation indicators are employed to assess the segmentation quality. The experimental results demonstrate that the SCGJO exhibits fantastic durability and stability to arrive at a faster convergence rate, higher calculation precision and greater segmentation accuracy.

The following sections make up this article. Section 2 explores multilevel thresholding. Section 3 describes GJO. Section 4 generates SCGJO. In Section 5, the

SCGJO-based multilevel threshold method is established. The experimental results and analysis are detailed in Section 6. Finally, conclusions and future research are explained in Section 7.

2 Multilevel thresholding

The purpose of image segmentation is to separate a given original image into several unusual and distinctive core regions and exhibit the principle and process of interested objects. The SCGJO has excellent robustness and reliability to acquire recognition accuracy and segmentation quality. The image thresholding segmentation mainly contains bi-level thresholding and multilevel thresholding. The bi-level thresholding is employed to tackle the simple image with the object and background, which necessitates identifying an optimal threshold value to determine the better segmentation quality and achieve the image segmentation. Multilevel thresholding is a pivotal unassisted image segmentation technique that selects multiple threshold values to classify and extract the interested parts. This method has certain superiority and dependability to deal with complicated image segmentation and obtain high segmentation precision.

Kapur's entropy based on the non-parametric thresholding technique separates the original image into multiple categories by contrasting the histogram's entropy value. A larger Kapur's entropy means that the segmentation categories are homogeneous, and this method is superior to other threshold segmentation methods. Kapur's entropy has distinctive advantages: low computational cost, simple implementation, fast operation speed, high segmentation precision, strong robustness and stability. The discreteness and compactness between various categories are reflected in the image's entropy. Kapur's entropy is a constructive method to address image segmentation, which has significant stability and resilience to determine the best segmentation quality [20]. Assuming that n threshold values from the best values $[t_1, t_2, \ldots, t_n]$ are utilized to separate the source image into distinct categories. The probability p_i is generated as:

$$p_i = \frac{h_i}{\sum_{i=0}^{L-1} h(i)} \tag{1}$$

where h_i denotes the pixel size, L denotes the level size.

Kapur's entropy is generated as:

$$f\left(t_1, t_2, \ldots, t_n\right) = H_0 + H_1 + H_2 + \cdots + H_n \tag{2}$$

where

$$H_0 = -\sum_{i=0}^{t_1-1} \frac{p_i}{\omega_0} \ln \frac{p_i}{\omega_0}, \omega_0 = \sum_{i=0}^{t_1-1} p_i \tag{3}$$

$$H_1 = -\sum_{i=t_1}^{t_2-1} \frac{p_i}{\omega_1} \ln \frac{p_i}{\omega_1}, \omega_1 = \sum_{i=t_1}^{t_2-1} p_i \tag{4}$$

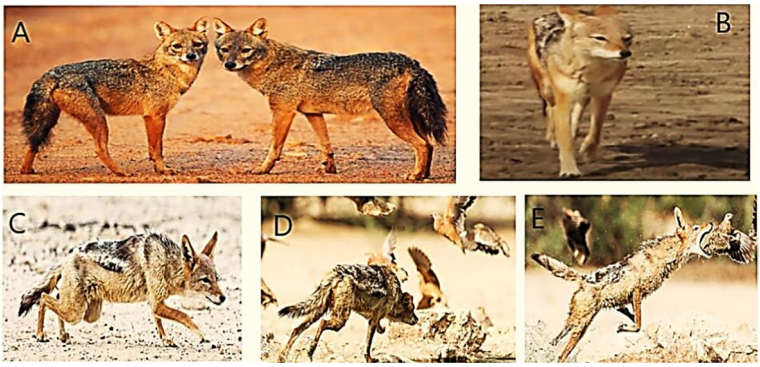

Fig. 1 **A** Jackal pair **B** Jackal discovering prey **C** Tracking and encircling of prey **D** & **E** Tapping prey

$$H_2 = -\sum_{i=t_2}^{t_3-1} \frac{p_i}{\omega_2} \ln \frac{p_i}{\omega_2}, \omega_2 = \sum_{i=t_2}^{t_3-1} p_i \tag{5}$$

$$H_n = -\sum_{i=t_n}^{L-1} \frac{p_i}{\omega_n} \ln \frac{p_i}{\omega_n}, \omega_n = \sum_{i=t_n}^{L-1} p_i \tag{6}$$

H_0, H_1, …, H_n denote the distinct categories' Kapur's entropies, ω_0, ω_1, …, ω_n denote the probabilities of each category.

3 GJO

The GJO involves three essential search operations: discovering prey, tracking and encircling prey, and trapping prey. The GJO utilizes these operations to regulate exploitation and exploration to determine the best value. Each jackal symbolizes a search agent. The jackal pair's foraging mechanism is shown in Fig. 1. The correlation between solution space and GJO space is shown in Table 1.

Table 1 Correlation between solution space and GJO space

Solution space	GJO space
Search space	Prey scope
Each solution	A golden jackal
Evaluation value of each solution	Objective value of GJO

3.1 Search space

In GJO, the candidate values are stochastically generated and uniformly distributed in the detection region, the purpose is to identify the overall best value from various search agents. The initial solution is generated as:

$$Y_0 = Y_{\min} + \text{rand}\left(Y_{\max} - Y_{\min}\right) \tag{7}$$

where $Y_{\max}$ and $Y_{\min}$ denote the variable's limit, *rand* denotes a haphazard vector in [0,1].

The first and second fittest is jackal pair, the matrix prey is generated as:

$$Prey = \begin{bmatrix} Y_{1,1} & Y_{1,2} & \cdots & Y_{1,d} \\ Y_{2,1} & Y_{2,2} & \cdots & Y_{2,d} \\ \vdots & \vdots & \vdots & \vdots \\ Y_{n,1} & Y_{n,2} & \cdots & Y_{n,d} \end{bmatrix} \tag{8}$$

where $Y_{i,j}$ denotes the *jth* dimension of *ith* prey, n denotes the population size, d denotes the issue dimension. The objective's matrix is generated as:

$$F_{OA} = \begin{bmatrix} f\left(Y_{1,1};Y_{1,2};Y_{1,d}\right) \\ f\left(Y_{2,1};Y_{2,2};Y_{2,d}\right) \\ \vdots \\ f\left(Y_{n,1};Y_{n,2};Y_{n,d}\right) \end{bmatrix} \tag{9}$$

where F_{OA} denotes a matrix that stores the objective values. A male jackal is considered to be the fittest, while a female jackal is considered to be the second fittest. In other words, the male jackal symbolizes the ideal fitness value whereas the female jackal symbolizes the suboptimal fitness value.

3.2 Exploration phase or discovering the prey

This section mainly describes the exploration phase of the GJO. Jackal has a distinctive nature to apperceive and track the prey, but contingently the prey followed by the golden jackal is not captured and easily escapes. The jackals watch patiently before swiftly seeking newly targeted prey. Female jackal accompanies male jackal to accomplish the hunting process. The positions are generated as:

$$Y_1(t) = Y_M(t) - E \cdot \mid Y_M(t) - rl \cdot Prey(t) \mid \tag{10}$$

$$Y_2(t) = Y_{FM}(t) - E \cdot \left|Y_{FM}(t) - rl \cdot Prey(t)\right| \tag{11}$$

where t denotes the current iteration, $\boldsymbol{Prey}(t)$ denotes the prey's position vector, $Y_M(t)$ and $Y_{FM}(t)$ denote the latest positions of the jackal pair, $Y_1(t)$ and $Y_2(t)$ denote the updated positions of the jackal pair.

The evading energy of prey E is generated as:

$$E = E_1 * E_0 \tag{12}$$

where E_1 denotes the prey's declining energy, E_0 denotes the energy's original status.

$$E_0 = 2 * r - 1 \tag{13}$$

where r denotes a haphazard value in [0,1].

$$E_1 = c_1 * (1 - (t/T)) \tag{14}$$

where T denotes the maximum iteration, c_1 denotes a constant that is set to 1.5, E_1 linearly decreases from 1.5 to 0.

The rl is a random vector with Lévy distribution, which is generated as:

$$rl = 0.05 * LF(y) \tag{15}$$

The LF is the fitness function, which is generated as:

$$LF(y) = 0.01 \times (\mu \times \sigma)/\left(|v^{(1/\beta)}|\right); \sigma = \left(\frac{\Gamma(1+\beta) \times \sin(\pi\beta/2)}{\Gamma\left(\frac{1+\beta}{2}\right) \times \beta \times \left(2^{\frac{\beta-1}{2}}\right)}\right)^{1/\beta} \tag{16}$$

where μ and v denote the haphazard values in (0,1), β denotes a constant that is set to 1.5.

The position of the golden jackal is generated as:

$$Y(t+1) = \frac{Y_1(t) + Y_2(t)}{2} \tag{17}$$

3.3 Exploitation phase or enclosing and pouncing on the prey

This section mainly describes the exploitation phase of the GJO. Once the target prey is discovered in the search region, the jackals will rapidly enclose and harass the prey. The evading energy of prey decay expeditiously, which causes the jackals to track and devour the prey. The foraging behavior of the jackal pair is generated as:

$$Y_1(t) = Y_M(t) - E \cdot \left|rl \cdot Y_M(t) - Prey(t)\right| \tag{18}$$

$$Y_2(t) = Y_{FM}(t) - E \cdot \left|rl \cdot Y_{FM}(t) - Prey(t)\right| \tag{19}$$

where Prey(t) denotes the position vector, $Y_M(t)$ and $Y_{FM}(t)$ denote the latest positions of the jackal pair, $Y_1(t)$ and $Y_2(t)$ denote the updated positions of the jackal pair. Finally, the position is generated as a formula (17).

The solution procedure of GJO is shown in Algorithm 1.

Algorithm 1 GJO

Begin
Step 1. Initialize the random prey population $Y_i(i = 1, 2, ..., n)$
Step 2. Calculate the fitness of each prey
Obtain the best prey (male jackal position) Y_1, the second best prey (female jackal position) Y_2
Step 3. while ($t < T$) do
for each prey
Update the evading energy E using Eqs. (12), (13) and (14)
Update rl using Eqs. (15) and (16)
if ($|E| \geq 1$)
Update the prey position using Eqs. (10), (11) and (17) based on exploration phase
else ($|E| < 1$)
Update the prey position using Eqs. (18), (19) and (17) based on exploitation phase
end if
end for
Check if any prey goes beyond the search space and amend it
Calculate the fitness of each prey
Update Y_1 if there is a better solution
$t = t + 1$
end while
return Y_1
End

4 SCGJO

The SCA is introduced into the basic GJO to eliminate premature convergence, inferior computation accuracy and sluggish convergence rate. The SCGJO is a constructive and efficacious method to address the image segmentation. The SCGJO not only exhibits fantastic robustness and reliability to promote the complementary benefits and boost the convergence accuracy but also integrates exploration and exploitation to mitigate premature convergence and arrive at the better segmentation quality.

4.1 SCA

The SCA utilizes the adaptive parameters and multiple random candidate solutions to achieve a balanced transformation between exploration and exploitation. The SCA has a substantial stability and optimization ability to mitigate search stagnation and determine the overall best value, which promotes the convergence rate and enhances the calculation precision. The position of the SCA is generated as:

$$X_i^{t+1} = \begin{cases} X_i^t + r_1 \times \sin\left(r_2\right) \times \mid r_3 P_i^t - X_i^t \mid, & r_4 < 0.5 \\ X_i^t + r_1 \times \cos\left(r_2\right) \times \mid r_3 P_i^t - X_i^t \mid, & r_4 \geq 0.5 \end{cases} \tag{20}$$

where X_i^t denotes the current position, X_i^{t+1} denotes the updated position, P_i^t denotes the best position in the search region, r_1, r_2, r_3, r_4 denote the haphazard values, $r_2 \in [0, 2\pi]$, $r_3 \in [-2, 2]$, $r_4 \in [0, 1]$, $\|$ denotes the absolute value.

The amplitude conversion factor r_1 is generated as:

$$r_1 = a - t \times \frac{a}{T} \tag{21}$$

where a denotes a constant.

4.2 SCGJO

In the exploration phase of the SCGJO, the positions are generated as:

$$Y_1'(t) = \begin{cases} Y_1(t) + r_1 \times \sin\left(r_2\right) \times \mid r_3 prey - Y_1(t) \mid, & r_4 < 0.5 \\ Y_1(t) + r_1 \times \cos\left(r_2\right) \times \mid r_3 prey - Y_1(t) \mid, & r_4 \geq 0.5 \end{cases} \tag{22}$$

$$Y_2'(t) = \begin{cases} Y_2(t) + r_1 \times \sin\left(r_2\right) \times \mid r_3 prey - Y_2(t) \mid, & r_4 < 0.5 \\ Y_2(t) + r_1 \times \cos\left(r_2\right) \times \mid r_3 prey - Y_2(t) \mid, & r_4 \geq 0.5 \end{cases} \tag{23}$$

$$Y(t+1) = \frac{Y_1'(t) + Y_2'(t)}{2} \tag{24}$$

where Prey(t) denotes the prey's position vector, $Y_1(t)$ and $Y_2(t)$ denote the latest positions of the jackal pair, $Y_1'(t)$ and $Y_2'(t)$ denote the updated positions of the jackal pair according to the SCA. $r_2 \in [0, 2\pi]$, $r_3 \in [-2, 2]$, $r_4 \in [0, 1]$, r_1 is linearly decreases from 2 to 0, Y denotes the updated position of the jackal.

In the exploitation phase of the SCGJO, the positions are generated as:

$$Y_1''(t) = \begin{cases} Y_1(t) + r_1 \times \sin\left(r_2\right) \times \mid r_3 prey - Y_1(t) \mid, & r_4 < 0.5 \\ Y_1(t) + r_1 \times \cos\left(r_2\right) \times \mid r_3 prey - Y_1(t) \mid, & r_4 \geq 0.5 \end{cases} \tag{25}$$

$$Y_2''(t) = \begin{cases} Y_2(t) + r_1 \times \sin\left(r_2\right) \times \mid r_3 prey - Y_2(t) \mid, & r_4 < 0.5 \\ Y_2(t) + r_1 \times \cos\left(r_2\right) \times \mid r_3 prey - Y_2(t) \mid, & r_4 \geq 0.5 \end{cases} \tag{26}$$

$$Y(t+1) = \frac{Y_1''(t) + Y_2''(t)}{2} \tag{27}$$

where Prey(t) denotes the prey's position vector, $Y_1(t)$ and $Y_2(t)$ denote the latest positions of the jackal pair, $Y_1''(t)$ and $Y_2''(t)$ denote the updated positions of the jackal pair according to the SCA. $r_2 \in [0, 2\pi]$, $r_3 \in [-2, 2]$, $r_4 \in [0, 1]$, r_1 is linearly decreases from 2 to 0, Y denotes the updated position of the jackal.

The solution procedure of SCGJO is shown in Algorithm 2.

Algorithm 2 SCGJO

Begin

Step 1. Initialize the random prey population $Y_i(i = 1, 2, ..., n)$

Step 2. Calculate the fitness of each prey

Obtain the best prey (male jackal position) Y_1, the second best prey (female jackal position) Y_2

Step 3. while ($t < T$) do

for each prey

Update the evading energy E using Eqs. (12), (13) and (14)

Update rl using Eqs. (15) and (16)

if $(|E| \geq 1)$

Combine SCA with exploration phase of GJO

Update the prey position of SCGJO using Eqs. (22), (23) and (24)

else $(|E| < 1)$

Combine SCA with exploitation phase of GJO

Update the prey position of SCGJO using Eqs. (25), (26) and (27)

end if

end for

Check if any prey goes beyond the search space and amend it

Calculate the fitness of each prey

Update Y_1 if there is a better solution

$t = t + 1$

end while

return Y_1

End

5 SCGJO-based multilevel threshold method

5.1 The solution procedure of the SCGJO

In SCGJO, the position of the jackal is equivalent to the image's segmentation threshold value. The jackal is employed to refresh the position, track and enclose, pounce on, and capture the prey according to the set threshold level, which promotes exploration and exploitation to determine the best value. The correlation between image segmentation and SCGJO is shown in Table 2. The solution procedure of SCGJO based on image segmentation is shown in Algorithm 3. The flowchart of SCGJO for multilevel thresholding is shown in Fig. 2.

Table 2 Correlation between image segmentation and SCGJO

Image segmentation	SCGJO
A set of all schemes $(n_1, n_2, \ldots, n_k)$ to tackle the image segmentation	A golden jackal population X with$(x_1, x_2, \ldots, x_k)$
The optimal scheme that achieves the best solution	The best golden jackal
The evaluation value of the image segmentation	The objective value of SCGJO

5.2 Computational complexity of the SCGJO

The computational complexity of the SCGJO is regarded as an objective value that directly connects the issue's input size to the algorithm's run-time. The big-O notation furnishes a trustworthy method to quantify and assess the algorithm's stability and validity. The computational complexity of the SCGJO is anatomized in detail.

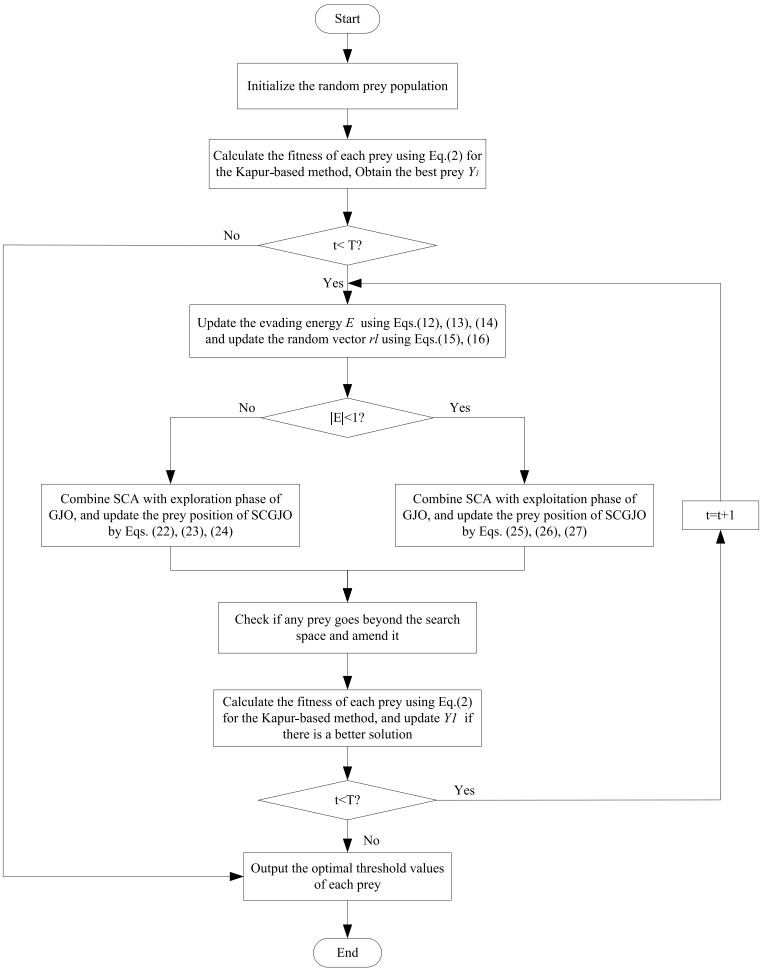

Fig. 2 Flowchart of SCGJO for multilevel thresholding

Algorithm 3 SCGJO based on image segmentation for Kapur entropy

Begin

Step 1. Initialize the random prey population $Y_i (i = 1, 2, ..., n)$

Step 2. Calculate the fitness of each prey using Eq. (2) for the Kapur-based method

Obtain the best prey (male jackal position) Y_1, the second best prey (female jackal position) Y_2

Step 3. while ($t < T$) do

for each prey

Update the evading energy E using Eqs. (12), (13) and (14)

Update rl using Eqs. (15) and (16)

if $(|E| \geq 1)$

Combine SCA with exploration phase of GJO

Update the prey position of SCGJO using Eqs. (22), (23) and (24)

else $(|E| < 1)$

Combine SCA with exploitation phase of GJO

Update the prey position of SCGJO using Eqs. (25), (26) and (27)

end if

end for

Check if any prey goes beyond the search space and amend it

Calculate the fitness of each prey using Eq. (2) for the Kapur-based method

Update Y_1 if there is a better solution

$t = t + 1$

end while

return the best prey Y_1, which denotes the optimal threshold values of segmentation

End

The SCGJO primarily involves three procedures: initialization, assessing the objective value and updating the golden jackal's position according to the exploration and exploitation. In SCGJO, N denotes the population size, T denotes the maximum iteration, and D denotes the issue dimension. The computational complexity of initialization is $O(N)$. For assessing the objective value and updating the golden jackal's position, the computational complexity is $O(T \times N) + O(T \times N \times D)$. The SCGJO not only has fantastic adaptability and reliability to promote the complementary benefits and boost the convergence accuracy but also integrates exploration and exploitation to mitigate search stagnation and determine the ideal value. Therefore, the computational complexity of the SCGJO is $O(N \times (T + T \times D + 1))$, the SCGJO is an effective and trustworthy approach to address the optimization issue.

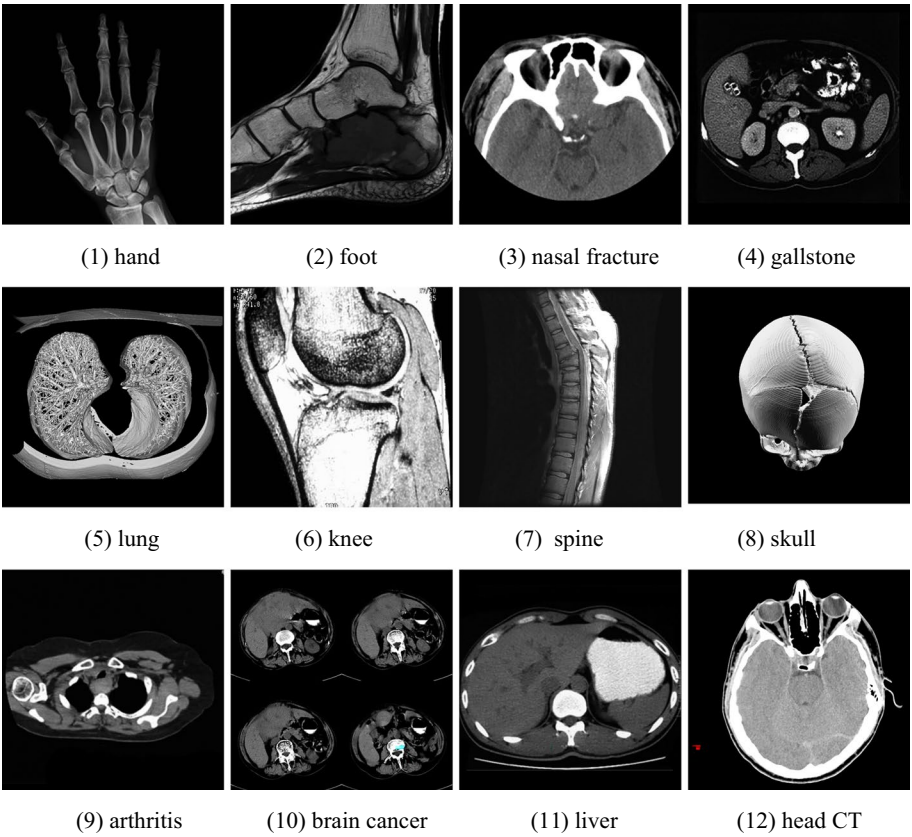

Fig. 3 Original test images

6 Experimental results and analysis

6.1 Experimental setup

The numerical experiment is implemented on a computer about an Intel Core i7-8750H 2.2 GHz CPU, a GTX1060, and 8 GB memory with Windows 10 system. All of the algorithms are programmed in MATLAB R2018b.

6.2 Test images

To verify the productivity and feasibility, the SCGJO is utilized to address the image segmentation, the experiments are conducted on twelve test images that are elaborately chosen from computerized tomography (CT) or magnetic resonance imaging (MRI) machines [40], and shown in Fig. 3.

6.3 Parameter setting

The SCGJO is contrasted with various algorithms to reveal the stability and superiority, such as BA, DOA, FPA, MFO, SCA and GJO. The algorithm's parameters are taken from the primary articles and are credible, typical empirical values, which are shown in Table 3.

6.4 Segmented image quality measurements

Six momentous evaluation indicators are applied to evaluate the segmentation quality, and further assess the stability and overall search ability. The evaluation indicators are generated as:

Table 3 Parameters of each algorithm

Algorithm	Parameter	Value
BA	Pulse frequency range f	[0,2]
	Echo loudness A	0.25
	Decreasing coefficient γ	0.5
DOA	Haphazard vector a_1	[0,1]
	Haphazard vector a_2	[0,1]
	Coefficient vector A	(1,0)
	Coefficient vector B	(1,1)
	Haphazard number b	(0,3)
FPA	Switch probability ρ	0.8
MFO	Constant b	1
	Haphazard value t	[−1,1]
	Haphazard value r	[−2,-1]
SCA	Constant a	2
	Haphazard value r_2	[0, 2π]
	Haphazard value r_3	[−2, 2]
	Haphazard value r_4	[0, 1]
GJO	Haphazard value *rand*	[0,1]
	Haphazard value r	[0,1]
	Constant value c_1	1.5
	Haphazard value u	(0,1)
	Haphazard value v	(0,1)
	Constant value β	1.5
SCGJO	Haphazard value *rand*	[0,1]
	Haphazard value r	[0,1]
	Constant value c_1	1.5
	Haphazard value u	(0,1)
	Haphazard value v	(0,1)
	Constant value β	1.5
	Constant a	2
	Haphazard value r_2	[0, 2π]
	Haphazard value r_3	[−2, 2]
	Haphazard value r_4	[0, 1]

(1) Fitness value. The convergence rate and calculation precision of the evolutionary algorithm are impacted by the fitness value, and whether it identifies the global best value. The intention is to actualize the accurate threshold values and the maximum objective values. The fitness value and the segmented image information are positively correlated. The segmented image involves more meaningful information since the algorithm's fitness value is greater.

(2) The best threshold value. The most effective threshold value setting is essential for image segmentation, which impacts the evaluation indicators and determines the segmentation quality. The evolutionary algorithm is utilized to address the image segmentation and arrive at the best threshold value. The intention is to realize the best threshold values and the maximum fitness values. The evolutionary algorithm has excellent durability and reliability to promote the segmentation's accuracy and quality.

(3) Execution time. For each algorithm, the population size is 30, the maximum iteration is 100, and the independent operation is 30. The threshold levels are defined as 4, 5, 6, 7 and 8 respectively. The execution time is an essential evaluation indicator to confirm the convergence speed and calculation accuracy. The evolutionary algorithm integrates exploration and exploitation to mitigate search stagnation and address the complex issues. The evolutionary algorithm consumes less time, which reveals that the algorithm had excellent resilience and search efficiency to identify the best solution.

(4) Peak signal to noise ratio (PSNR). The PSNR, a typical indicator to recognize signal distortion, is a ratio of the greatest potential power expressing a signal to the strength of destructive noise that impacts the accuracy of its representation. The PSNR utilizes the intensity value of a given image to determine whether is a certain difference before and after image segmentation. The PSNR is based on the image pixel gray value to analyze the algorithm performance and evaluate the segmentation quality. A higher PSNR value indicates the segmented image exhibits less distortion and greater segmentation quality. Since the visual properties of the human eye are not taken into account, this will cause inconsistency between people's subjective sensations and evaluation results. The PSNR is generated as [1]:

$$PSNR = 10\log_{10}\left(\frac{255^2}{MSE}\right) \tag{28}$$

where MSE denotes the average squared error. The MSE is generated as:

$$MSE = \frac{1}{MN}\sum_{i=1}^{M}\sum_{j=1}^{N}\left[I(i,j) - K(i,j)\right]^2 \tag{29}$$

where $M \times N$ denotes the image size, $I(i,j)$ denotes the source image, $K(i,j)$ denotes the segmented image.

(5) Structural similarity index (SSIM). The SSIM estimates the similarity between the source image and the segmented image, which defines structural information to maintain the scene object's structure independently of brightness and contrast. Brightness, contrast, and structure are three separate elements that are combined

to describe the distortion. The pixel means is employed to assess brightness, the standard deviation is required to evaluate contrast, and the covariance is utilized as a measure of structural similarity. The SSIM is a random number between 0 and 1. The discrepancy between the source image and the segmented image is diminished, and the segmentation quality is enhanced as the threshold level rises. The SSIM is generated as [39]:

$$SSIM(x,y) = \frac{\left(2\mu_x\mu_y + c_1\right)\left(2\sigma_{xy} + c_2\right)}{\left(\mu_x^2 + \mu_y^2 + c_1\right)\left(\sigma_x^2 + \sigma_y^2 + c_2\right)} \tag{30}$$

where μ_x and μ_y denote the average intensity before and after image segmentation respectively. σ_x^2 and σ_y^2 denote the standard deviation before and after image segmentation respectively. σ_{xy} denotes the covariance before and after image segmentation. c_1 and c_1 denote constants.

(6) Wilcoxon's rank-sum test. Wilcoxon's rank-sum test [8] is employed to confirm if there is a substantial disparity between the two groups of data, which is an important evaluation indicator to verify the effectiveness and disparity. $p < 0.05$ implies that there is a substantial disparity between the SCGJO and other algorithms. $p \geq 0.05$ implies that there is no substantial disparity between the SCGJO and other algorithms.

6.5 Results and analysis

For each algorithm, the population size is 30, the maximum iteration is 100, and the independent operation is 30. The threshold levels are defined as 4, 5, 6, 7 and 8 respectively. The experimental results of the SCGJO are contrasted with those of BA, DOA, FPA, MFO, SCA, and GJO in Tables 4-9.

The optimal fitness of each algorithm is shown in Table 4. Various evolutionary algorithm is employed to address image segmentation, which utilizes entropy quantization to assess the segmented information and maximize the entropy of the target or background regions. The intention is to actualize the accurate threshold values and the maximum fitness values according to certain optimization criteria. The optimal fitness of each algorithm enlarges as the threshold level enlarges, which illustrates that the segmented image exhibits a greater segmentation impact and incorporates more segmentation information. To demonstrate the superiority and stability of the algorithms, twelve images with five different threshold levels are employed to assess the segmentation quality. The optimal fitness values of the SCGJO are superior to those of BA, DOA, FPA, MFO, SCA, and GJO. The ranking of the SCGJO based on the optimal fitness value is the first, which illustrates that the SCGJO has excellent stability to determine the best value. The best threshold values of each algorithm are shown in Table 5. The threshold values can affect the rest of the evaluation indicators and determine the image segmentation quality. The SCGJO with better threshold values has a greater overall search performance to arrive at the segmented image with higher segmentation accuracy and

Table 4 The optimal fitness of each algorithm

Images	k	Optimal fitness values							
		BA	DOA	FPA	MFO	SCA	GJO	SCGJO	Rank
Test 1	4	15.5655	15.6502	15.4989	15.5147	15.3681	15.4093	15.6860	1
	5	18.2197	18.1300	18.3461	18.3296	17.9523	18.2753	18.4295	1
	6	20.5234	20.6237	20.5631	20.5237	20.7369	20.4260	20.7454	1
	7	22.6238	22.5428	22.6940	22.6986	22.7155	22.5045	22.8442	1
	8	24.8008	24.9792	24.9684	24.8775	25.2493	25.0765	25.3041	1
Test 2	4	17.6290	17.7831	17.8813	17.9016	18.0169	18.0287	18.0556	1
	5	20.6343	20.7125	20.2480	20.7060	20.5047	20.6472	20.7720	1
	6	23.1094	22.9366	22.8936	23.0736	22.8281	22.8679	23.2467	1
	7	25.4090	25.7545	24.9857	25.3169	25.6536	25.0621	25.8939	1
	8	27.1829	27.7401	27.9150	27.4945	27.3621	27.8938	28.0256	1
Test 3	4	14.0372	14.1877	14.4048	14.5729	14.2460	14.1395	14.8042	1
	5	16.8308	17.0728	16.8785	17.0754	16.9704	16.9169	17.1395	1
	6	19.0725	19.1346	19.5356	19.7826	19.4664	19.7032	19.7859	1
	7	21.7106	21.8720	22.0059	21.8479	21.7315	22.4505	22.6460	1
	8	24.5471	24.3546	24.2407	24.5577	24.5411	24.6969	24.6975	1
Test 4	4	17.3665	17.2138	17.3497	17.3502	17.3236	17.2193	17.4950	1
	5	20.0514	20.2688	20.3378	20.1278	20.1979	20.0413	20.3601	1
	6	22.5405	22.7530	22.6991	22.7253	22.7590	22.9596	23.0615	1
	7	25.1794	25.2589	24.9628	25.4148	25.2005	25.1818	25.4429	1
	8	27.8643	27.8048	27.5623	27.7642	27.3089	27.8028	28.1633	1
Test 5	4	15.7654	15.7897	15.5797	15.6505	15.6768	15.4646	16.1581	1
	5	18.5377	18.1918	18.4922	18.1995	18.4288	18.5163	18.5430	1
	6	20.7311	21.0792	20.7964	21.0786	20.9053	21.1974	21.2465	1
	7	23.5760	23.6212	23.5724	23.7152	23.2765	23.3094	23.8611	1
	8	25.8778	26.0251	26.1438	26.2069	26.1709	26.0030	26.3488	1
Test 6	4	17.4124	17.3026	17.0686	17.0923	17.3576	17.2115	17.5056	1
	5	19.7399	19.8742	19.9092	19.5525	19.7581	20.1296	20.1803	1
	6	22.3865	22.3733	22.2857	22.1458	22.2458	22.0647	22.3967	1
	7	24.6470	24.7082	24.2427	24.6147	24.5887	24.4800	24.8607	1
	8	27.2068	27.1215	27.1154	27.2022	26.9807	26.9413	27.3343	1
Test 7	4	16.2507	16.4151	16.8860	16.8369	16.5457	16.9071	16.9789	1
	5	19.4167	18.9102	18.8984	19.3054	19.7017	19.1399	19.8613	1
	6	21.6250	21.5271	21.9357	21.7370	22.2306	21.4939	23.4919	1
	7	23.8688	23.8127	23.5915	23.8923	25.5166	23.8281	26.8513	1
	8	25.7454	26.5530	26.1186	26.5392	28.8717	26.4027	29.9190	1
Test 8	4	15.4654	15.7459	15.7623	15.7458	15.6765	15.6899	15.7913	1
	5	18.1741	18.0484	17.9791	18.2454	18.0621	18.2672	18.3900	1
	6	21.0702	20.7942	20.8006	20.9109	21.1763	21.0454	21.2243	1
	7	23.2746	23.0211	22.9147	22.8813	23.5836	23.4829	23.8656	1
	8	25.4456	25.7127	25.7853	25.7449	25.3272	25.7933	25.8247	1
Test 9	4	17.0584	17.0009	16.7636	16.9446	16.9429	16.6835	17.3156	1
	5	19.6969	19.8786	19.8066	19.8083	19.8028	19.5759	20.1413	1
	6	22.6193	21.9898	22.2330	21.9557	22.5645	22.3219	22.6303	1

Table 4 (continued)

Images	k	Optimal fitness values							
		BA	DOA	FPA	MFO	SCA	GJO	SCGJO	Rank
	7	24.9340	24.7039	24.5853	24.8843	24.7492	24.6853	25.0326	1
	8	26.7275	27.1425	27.2024	26.9395	26.5717	26.8242	27.3266	1
Test 10	4	16.1097	16.0937	15.8859	15.9841	15.9903	15.8760	16.1154	1
	5	18.7332	18.9253	18.6423	18.6862	18.6296	18.7492	19.0454	1
	6	21.3064	21.4169	21.2355	21.2586	21.4304	21.3256	21.7506	1
	7	24.1977	23.7162	23.8950	23.8829	24.1592	23.9410	24.2421	1
	8	26.5033	25.9750	26.3069	26.1241	26.0879	26.3278	26.6034	1
Test 11	4	17.6200	17.6261	17.3976	17.3138	17.1213	17.3131	17.7993	1
	5	19.8319	20.0661	20.2756	20.0190	20.2924	20.1035	20.3930	1
	6	22.5475	22.6425	22.1196	22.6705	22.3241	22.3889	22.8979	1
	7	24.9962	24.9691	24.9685	24.9042	24.7827	24.7946	25.0427	1
	8	26.9982	26.7531	27.1012	27.2434	27.2371	27.3743	27.6572	1
Test 12	4	11.1829	11.8470	11.6645	11.7663	11.73859	11.7505	11.8507	1
	5	13.6704	13.6421	13.7556	13.0592	13.0352	13.1952	13.8440	1
	6	15.0846	14.8544	15.0052	14.9497	14.9965	15.1521	15.1905	1
	7	16.6044	16.8417	17.0065	16.6992	16.8934	16.3495	17.0338	1
	8	18.5201	18.2946	18.3054	18.6989	18.2343	18.1475	18.7885	1

quality. The SCGJO utilizes the collaborative foraging mechanism of discovering prey, tracking and enclosing prey, and pouncing on prey. The SCGJO not only has excellent exploration and exploitation to determine the ideal value but also achieves complementary benefits to promote convergence accuracy and segmentation quality. The SCGJO is an effectual and constructive method for addressing the image segmentation.

The average execution time of each algorithm is shown in Table 6. For each algorithm, the population size is 30, the maximum iteration is 100, and the independent operation is 30. The execution time is an essential evaluation indicator to confirm the convergence speed and calculation accuracy. The threshold level is larger, and the execution time and the computational complexity of each algorithm gradually increase, which illustrates that the evolutionary algorithm consumes more execution time. The SCGJO has significant stability and resilience to arrive at the best fitness value and threshold value. The SCGJO combines the advantages of the SCA and GJO to promote the optimization ability, mitigate search stagnation and actualize the accurate segmentation quality. However, the SCGJO consumes more execution time to accomplish the image segmentation compared to the GJO and SCA. The experimental results demonstrate that the SCGJO utilizes exploration or exploitation to acquire a higher convergence accuracy and greater segmentation quality.

The PSNR of each algorithm based on Kapur's entropy method is shown in Table 7. The PSNR, a typical indicator to detect signal distortion, is a ratio of the

Table 5 The best threshold values of each algorithm

Images	k	Best threshold values						
		BA	DOA	FPA	MFO	SCA	GJO	SCGJO
Test 1	4	11,62,116,153	34,73,126,160	52,79,130,171	48,94,119,165	23,66,148,175	6,73,106,147	11,61,105,170
	5	15,63,92,145, 185	27,84,104,141, 180	7,39,73,110, 175	14,62,102,144, 166	42,75,117,147, 162	19,50,103,135, 181	9,43,71,116, 164
	6	12,64,98,134, 153,195	13,35,77,107, 164,181	20,54,103,124, 159,172	19,77,100,142, 161,190	15,52,83,98, 177	19,38,90,130, 159,171	6,24,79,117, 157,181
	7	14,38,78,131, 151,181,195	27,38,72,94, 113,133,158	12,63,111,130, 155,176,198	31,49,78,95, 127,173,196	16,37,81,91, 128,166,185	10,37,60,103, 157,177,186	18,49,73,90, 116,172,195
	8	14,20,39,61, 86,119,162,189	15,32,48,80, 111,143,152,188	9,35,48,58, 82,128,146,172	9,29,49,58, 84,129,156,197	10,33,64,83, 100,130,159,200	12,32,65,86, 94,128,156,174	9,30,51,79, 95,128,143,163
Test 2	4	24,83,119,173	37,70,114,192	60,88,131,189	69,108,148,199	50,117,163,207	41,89,133,202	48,104,152,186
	5	34,73,141,168, 189	43,70,142,172, 223	63,119,174,212, 232	31,56,113,153, 186	32,116,153,176, 226	29,56,109,157, 221	53,80,122,164, 195
	6	39,105,131,168, 203,218	25,74,125,179, 195,225	41,78,134,159, 168,200	44,85,96,137, 174,200	57,90,119,139, 200,238	51,83,123,137, 158,225	28,48,91,156, 194,223
	7	36,69,128,159, 175,206,217	26,53,87,106, 141,184,233	45,73,131,169, 211,221,242	30,48,68,106, 135,157,234	29,44,63,99, 144,186,231	51,73,91,116, 158,170,190	31,51,81,122, 164,184,209
	8	30,91,98,115, 162,184,206,234	32,57,73,132, 156,182,224,245	33,78,99,146, 163,199,218,238	62,76,92,125, 154,194,216,235	26,71,106,118, 154,161,194,229	59,93,120,144, 161,192,217,238	27,43,74,95, 129,141,173,217
Test 3	4	32,72,128,168	107,126,162,184	73,148,230,241	95,142,175,206	50,108,171,227	83,117,142,190	123,164,205,229
	5	72,114,160,202, 247	6,73,108,148, 214	46,81,112,175, 211	31,73,143,174, 227	86,117,141,179, 204	25,74,115,158, 187	8,60,102,156, 216
	6	8,43,54,140, 165,226	36,58,85,129, 153,194	30,83,103,148, 183,217	6,47,72,141, 178,212	19,46,81,142, 181,208	23,74,108,132, 195,221	27,75,120,174, 196,223
	7	12,49,107,155, 193,220,227	11,59,98,135, 182,198,234	14,39,70,100, 134,197,240	35,56,84,117, 142,182,202	23,54,70,121, 134,173,199	20,53,81,109, 128,171,222	11,55,75,113, 141,194,227
	8	28,59,98,117, 156,176,202,246	13,29,74,124, 143,184,205,222	28,44,90,105, 141,155,183,228	6,20,45,64, 97,158,188,228	17,42,71,110, 146,168,228,249	13,34,76,90, 113,149,177,224	9,46,80,132, 147,173,189,226
Test 4	4	17,90,169,230	31,110,147,181	41,78,132,202	29,73,160,226	20,92,138,229	37,110,147,240	50,113,170,232
	5	48,127,162,202, 233	28,57,94,144, 202	38,89,122,174, 235	11,59,101,174, 239	22,79,148,199, 229	38,64,88,148, 220	21,56,116,161, 202

Table 5 (continued)

Images	k	Best threshold values						
		BA	DOA	FPA	MFO	SCA	GJO	SCGJO
	6	17,76,115,163, 183,202	19,55,135,160, 207,230	18,64,141,160, 193,228	39,95,139,153, 197,234	34,80,112,161, 200,216	38,73,134,170, 207,238	30,65,101,132, 156,221
	7	18,50,77,114, 161,211,248	13,54,99,117, 167,220,244	36,54,130,152, 176,210,240	20,58,72,96, 133,186,229	26,71,86,105, 140,162,219	21,76,86,112, 143,191,226	8,50,73,104, 144,171,212
	8	10.47,79,101, 120,141,162,221	27,40,69,92, 126,174,209,236	11,39,58,113, 128,172,196,218	12,42,65,79, 124,170,216,242	15,64,93,109, 139,197,226,248	40,70,93,118, 155,194,222,243	17,45,66,84, 113,142,177,224
Test 5	4	19,56,106,187	20,63,129,189	22,54,137,213	21,84,138,194	26,66,107,175	53,107,147,218	3,55,113,172
	5	13,52,118,160, 230	17,70,115,140, 227	7,49,67,137, 197	8,28,88,117, 198	6,42,132,153, 186	8,83,118,184, 218	13,68,107,171, 202
	6	23,34,63,101, 139,193	13,39,63,87, 117,160	22,48,91,149, 185,237	6,30,86,109, 136,200	7,45,58,104, 128,210	23,61,84,108, 168,214	15,65,109,149, 185,206
	7	15,39,69,115, 139,188,235	7,33,59,75, 135,191,211	16,56,87,99, 124,162,195	6,26,39,64, 117,154,214	20,31,63,80, 114,151,217	6,43,61,118, 176,191,206	8,47,72,111, 153,167,225
	8	11,81,109,129, 157,192,218,243	10,62,72,89, 124,150,186,221	6,33,46,87, 112,130,178,207	8,31,66,98, 116,156,183,199	15,41,60,92, 104,133,186,217	8,53,79,121, 158,193,214,221	9,27,45,84, 112,137,171,208
Test 6	4	58,113,174,211	50,117,153,218	26,77,111,176	76,124,140,188	37,82,152,194	85,126,181,230	70,116,161,196
	5	39,75,129,193, 241	45,107,142,163, 188	48,91,138,178, 239	31,68,112,127, 202	55,85,150,209, 236	49,106,153,180, 212	60,103,151,191, 219
	6	25,50,89,121, 183,230	49,68,114,171, 196,236	39,55,76,111, 177,215	12,58,99,126, 179,216	19,54,87,127, 147,199	18,52,98,141, 164,184	27,51,116,160, 192,232
	7	28,43,80,125, 180,217,235	38,93,137,174, 189,209,240	7,54,74,91, 128,163,191	45,79,131,152, 192,210,221	33,66,116,136, 164,223,247	43,57,75,107, 132,167,237	49,72,106,137, 177,188,216
	8	33,50,66,113, 136,153,185,222	61,82,112,124, 146,176,199,220	35,46,72,92, 143,163,196,223	45,79,109,122, 136,173,206,235	33,62,105,121, 167,202,219,231	51,97,114,135, 150,188,207,222	39,58,79,92, 126,151,183,223
Test 7	4	61,93,150,169	36,75,108,195	24,78,129,164	39,86,125,171	28,89,121,132	32,81,121,160	26,71,115,161
	5	23,79,113,146, 168	38,105,155,197, 221	71,109,140,172, 199	30,81,121,176, 198	29,104,105,154, 248	38,52,90,130, 166	24,86,116,142, 194
	6	49,81,105,126, 151,196	25,88,106,141, 192,225	26,47,74,124, 169,194	25,80,127,145, 181,204	20,65,107,115, 171,235	26,59,101,166, 183,226	24,77,92,107, 146,168

Table 5 (continued)

Images	k	Best threshold values						
		BA	DOA	FPA	MFO	SCA	GJO	SCGJO
	7	37,56,104,146, 161,195,227	35,67,93,109, 155,203,217	31,72,99,153, 189,231,242	27,78,128,148, 172,188,205	38,85,115,124, 147,199,238	41,78,100,115, 147,174,187	25,45,92,115, 145,189,231
	8	28,75,114,129, 146,160,169,210	31,50,70,90, 122,154,187,228	44,63,86,109, 124,173,197,226	25,70,93,123, 152,180,192,221	21,48,60,86, 128,154,216,228	22,35,67,107, 129,151,175,212	24,35,72,108, 116,158,177,244
Test 8	4	53,98,150,185	32,96,141,193	6,85,153,196	25,78,157,203	12,79,117,196	22,70,104,172	13,61,113,197
	5	6,46,95,155, 172	15,52,105,186, 198	26,113,142,161, 219	17,49,111,160, 229	23,38,84,117, 163	10,33,73,149, 197	25,52,86,136, 171
	6	35,57,97,130, 160,212	14,32,87,123, 198,215	25,45,82,118, 136,176	32,68,116,140, 183,200	8,57,83,113, 139,203	7,33,63,104, 177,214	13,68,112,153, 184,228
	7	13,48,69,94, 106,134,196	22,72,110,118, 138,177,223	9,21,92,111, 153,175,212	7,66,140,154, 186,202,219	19,42,57,84, 113,151,208	14,30,65,115, 156,174,225	16,55,91,135, 157,200,221
	8	26,38,64,91, 112,154,180,194	22,47,79,112, 153,161,196,216	13,42,61,78, 127,160,197,233	13,33,76,109, 141,173,215,223	26,42,60,99, 119,176,213,230	25,60,85,101, 146,167,182,207	22,35,59,78, 100,126,158,201
Test 9	4	25,69,138,228	41,76,128,224	64,124,146,209	34,94,150,230	35,102,137,181	16,60,123,193	28,75,128,188
	5	22,75,113,186, 230	43,83,139,165, 220	44,89,128,155, 230	41,68,115,160, 199	34,104,126,175, 220	44,67,120,143, 188	26,61,124,172, 223
	6	36,89,132,179, 216,237	55,92,144,179, 221,236	27,90,111,164, 194,215	43,56,87,118, 186,214	32,78,124,184, 219,242	39,102,132,181, 215,236	39,79,113,149, 149,185,238
	7	9,29,57,83, 136,175,214	15,55,90,134, 170,192,213	22,85,126,148, 200,222,248	35,81,118,128, 161,193,232	29,47,96,131, 189,203,233	38,53,93,111, 138,188,212	21,83,122,146, 166,203,237
	8	32,45,69,102, 141,151,174,226	20,73,119,149, 169,192,224,244	32,84,118,130, 151,195,218,240	6,38,65,104, 145,191,208,247	36,89,98,131, 154,179,228,242	39,50,67,89, 131,147,193,224	17,33,67,98, 126,174,214,245
Test 10	4	88,130,173,211	6,52,139,187	29,64,144,224	8,81,152,207	39,138,175,219	11,54,160,206	16,82,124,179
	5	53,86,142,177, 228	12,69,144,186, 213	22,53,78,124, 164	51,98,130,201, 236	6,95,135,183, 205	19,59,148,199, 233	19,82,123,179, 216
	6	25,81,137,165, 179,209	16,38,70,121, 154,184	29,62,110,124, 186,226	18,69,92,159, 197,237	6,43,88,120, 136,204	22,98,123,141, 189,224	20,66,87,132, 185,223
	7	12,38,79,138, 182,211,230	7,40,66,114, 161,221,240	21,42,63,100, 149,190,218	16,57,80,115, 171,191,236	22,59,85,105, 143,184,220	12,46,88,130, 141,188,240	10,43,78,129, 186,208,242

Table 5 (continued)

Images	k	Best threshold values						
		BA	DOA	FPA	MFO	SCA	GJO	SCGJO
	8	14,59,84,127, 161,172,209,237	10,41,76,138, 147,170,185,218	15,33,74,101, 118,133,173,199	14,37,92,125, 152,204,221,232	36,70,102,116, 142,158,207,231	21,33,50,90, 127,169,209,243	29,54,93,115, 142,161,192,230
Test 11	4	110,151,185,226	96,131,178,213	56,101,170,210	45,107,150,209	102,112,144,190	67,114,172,194	100,152,196,228
	5	59,93,141,193, 212	19,52,102,178, 230	66,98,124,155, 196	107,124,155,197, 221	32,63,103,149, 194	14,38,105,146, 203	14,53,98,135, 192
	6	9,38,92,130, 178,220	23,52,115,143, 168,196	15,52,66,98, 154,173	16,42,105,133, 188,209	6,33,77,123, 168,205	19,78,102,139, 176,234	9,56,105,132, 181,210
	7	17,56,77,118, 167,187,226	30,69,98,142, 180,219,234	40,63,95,129, 171,211,231	7,35,60,88, 136,172,197	28,48,67,96, 130,151,211	14,76,114,138, 164,187,213	19,62,97,110, 160,205,225
	8	25,36,56,92, 119,139,200,224	61,76,119,146, 164,186,210,235	29,55,115,147, 169,179,200,229	10,69,83,108, 130,163,187,220	21,58,89,98, 124,176,194,217	15,53,72,102, 130,193,207,238	20,56,101,131, 160,179,191,229
Test 12	4	31,52,127,174	10,50,76,110	18,43,124,151	13,48,122,169	30,64,108,154	36,82,109,142	26,78,129,156
	5	9,55,73,126, 179	13,52,67,133, 173	12,80,100,134, 176	42,94,109,131, 170	19,75,102,135, 142	24,38,76,105, 168	14,34,85,138, 158
	6	16,39,75,99, 133,204	21,44,87,118, 176,195	11,44,93,118, 172,185	16,47,86,138, 214,241	15,40,66,99, 146,206	8,29,74,129, 192,213	7,53,102,124, 195,239
	7	15,47,85,93, 135,171,198	21,72,95,126, 148,199,239	9,20,41,69, 111,125,159	9,43,83,130, 144,157,203	28,59,100,135, 163,206,246	13,47,99,113, 125,172,208	6,51,87,121, 171,187,213
	8	13,31,64,108, 148,161,192,247	12,25,53,65, 135,185,214,243	12,28,72,134, 173,209,219,245	16,68,98,110, 133,181,215,242	24,33,57,93, 145,173,203,247	11,53,92,101, 139,155,192,206	7,27,59,108, 150,175,192,230

Table 6 The average execution time of each algorithm

Images	k	Execution time (in second)						
		BA	DOA	FPA	MFO	SCA	GJO	SCGJO
Test 1	4	2.7127	2.6124	2.6964	2.4082	2.2642	2.0737	3.0058
	5	2.7968	2.5935	2.7477	2.5089	2.3525	2.6484	3.1947
	6	3.0021	2.6616	3.3773	2.7941	2.5356	2.8502	3.2958
	7	3.1151	2.9367	3.0748	2.6786	2.5851	3.1332	3.4155
	8	3.4626	3.0377	3.1696	2.9156	2.8299	3.0877	3.6336
Test 2	4	3.0085	2.6517	2.8494	2.5556	2.5176	2.7849	3.1718
	5	2.9871	2.9287	2.8752	2.6906	2.7688	2.8221	3.4813
	6	3.3664	3.2438	2.8869	2.8157	2.6047	2.8577	3.7926
	7	3.1225	2.8774	2.9636	2.8726	2.6482	2.9645	3.8075
	8	3.3460	2.7659	2.9833	3.0424	2.7117	2.9433	3.8388
Test 3	4	2.8229	2.7576	2.8524	2.8429	2.7711	2.6765	3.0611
	5	3.0054	2.9868	2.8528	2.6827	2.5701	2.8373	3.1234
	6	3.1449	2.7561	2.9363	2.8397	2.7219	2.8908	3.2749
	7	3.3263	2.7709	2.9656	2.9177	2.6652	2.9211	3.4527
	8	3.3280	2.7601	2.9667	2.9242	2.7134	3.0445	3.4981
Test 4	4	2.8711	2.6161	2.7489	2.5838	2.4163	2.7453	3.0499
	5	3.1133	2.6881	2.9284	2.8493	2.5193	2.8285	3.0523
	6	3.1440	2.6994	3.2148	2.8308	2.9097	3.0748	3.1068
	7	3.3120	2.7049	2.9182	2.8561	2.6007	2.8333	3.2643
	8	3.2432	2.7581	3.0028	2.8285	2.7547	2.9336	3.2761
Test 5	4	2.9551	2.7161	2.9293	2.7634	2.4719	2.7426	3.0396
	5	3.2425	2.8194	2.8676	2.8465	2.6546	3.1323	3.1677
	6	3.0421	2.7882	3.3771	2.8765	2.6149	3.0699	3.1758
	7	3.2023	2.8198	2.9759	2.8700	2.6607	2.9355	3.6957
	8	3.3142	2.9734	2.9188	2.9927	2.7110	2.9374	3.8271
Test 6	4	2.9970	2.8485	2.8107	2.9936	2.5466	2.7524	3.0185
	5	3.0966	2.7244	2.8815	2.7585	2.6348	2.8023	3.0577
	6	3.5152	3.0258	2.8471	3.1099	2.7114	2.9031	3.3942
	7	3.5024	2.7991	2.8799	2.9503	2.7509	3.3666	3.6835
	8	3.6305	2.8442	3.0045	2.9557	3.2255	3.0212	3.7317
Test 7	4	2.7827	2.5924	2.8496	2.8928	2.3192	2.8468	3.0844
	5	2.9320	2.6918	2.8590	2.7370	2.5724	2.7049	3.1606
	6	2.9490	2.7578	2.9232	2.8521	2.8059	2.7709	3.1967
	7	2.9842	3.0216	2.9444	2.8092	2.9121	2.7969	3.3909
	8	3.0496	2.7240	2.9748	2.9338	3.0655	2.8115	3.4087
Test 8	4	2.9537	2.7330	2.8129	2.7064	2.4790	2.6409	3.0889
	5	3.1236	2.7727	2.8129	2.9787	2.5554	2.8350	3.1411
	6	3.2662	3.0842	2.8645	2.8193	2.6342	2.8331	3.2975
	7	3.1854	3.0590	2.8872	2.8281	2.6411	2.8820	3.3827
	8	3.5195	2.8178	3.3390	2.8721	2.8805	2.9337	3.6658
Test 9	4	2.9773	2.7005	2.7962	2.7935	2.3285	2.6779	3.1167
	5	3.0772	2.6933	2.7869	2.6055	2.5122	2.7284	3.2961
	6	3.3014	2.7587	2.8863	3.1811	2.5667	2.8163	3.3503

Table 6 (continued)

Images	k	Execution time (in second)						
		BA	DOA	FPA	MFO	SCA	GJO	SCGJO
	7	3.2109	2.7627	3.1539	2.7011	2.8126	2.8169	3.5214
	8	3.3941	2.9048	3.1744	2.7785	2.8235	2.8794	3.6368
Test 10	4	2.9502	2.8225	2.8638	2.8275	3.1275	2.8276	3.2239
	5	3.1191	2.7832	2.9292	2.7857	2.5332	2.8200	3.3255
	6	3.1188	2.8019	2.8810	2.8623	2.7126	2.8997	3.4927
	7	3.1505	2.8394	2.8741	2.9034	2.5976	2.9736	3.6655
	8	3.2783	2.8433	2.9026	2.8932	2.7674	3.2315	3.8114
Test 11	4	2.9148	2.6583	2.9148	2.6343	2.4272	2.6660	3.0963
	5	3.0425	2.9386	2.8507	2.8037	2.5108	2.9199	3.1774
	6	3.1580	2.7460	3.0394	2.7589	2.6375	2.8351	3.4003
	7	3.3514	3.1661	2.9757	2.9687	2.8026	3.1064	3.5795
	8	3.1863	2.7757	3.0281	3.1937	2.7450	2.9634	3.9781
Test 12	4	2.1625	2.6002	2.4230	2.4017	1.8989	2.5446	3.0626
	5	2.5996	2.6373	2.4710	2.4452	1.9796	2.3269	3.1183
	6	2.6054	2.2781	2.5014	2.0871	2.0657	2.6155	3.2849
	7	2.6958	2.7824	2.4752	2.6461	2.0387	2.4198	3.2963
	8	2.8743	2.3410	2.7260	2.6861	2.0294	2.4741	3.4659

signal's greatest potential intensity to the strength of destructive noise that impacts the representation accuracy. The PSNR value is calculated by the discrepancy between the associated elements, which is an error-sensitive indicator to assess the segmentation quality. The image segmentation accuracy is proportional to the threshold level. A higher PSNR value indicates the segmented image has less distortion, greater segmentation quality, and better convergence accuracy. The PSNR based on the intensity value is viewed to be an essential assessment indicator to reveal the discrepancy between the source image and segmented image, and then assess the distortion degree and the segmentation quality. For the PSNR values, the SCGJO based on Kapur's entropy are superior to those of the BA, DOA, FPA, MFO, SCA, and GJO according to the various threshold levels, which illustrates that the SCGJO has excellent stability and feasibility to address the image segmentation. As the threshold levels rise, the evolutionary algorithms' PSNR values rise proportionately. To verify the segmentation accuracy and convergence efficiency of the SCGJO, the PSNR value is employed to determine the ranking, the SCGJO has a higher ranking and a superior PSNR value, which illustrates that the SCGJO has sufficient predictability and reliability to attain better segmentation accuracy. There are 60 PSNR values for each algorithm, and the 50 PSNR values of the SCGJO are the best compared to other algorithms. The segmentation quality of the SCGJO is superior to those of other algorithms. The SCGJO not only combines the advantages of the SCA and GJO to mitigate search stagnation but also integrates exploration and exploitation to determine the better segmentation quality, which is an efficacious and realistic approach to address the image segmentation.

Table 7 The PSNR of each algorithm

Images	k	PSNR values							
		BA	DOA	FPA	MFO	SCA	GJO	SCGJO	Rank
Test 1	4	50.3109	49.9516	49.7412	49.7872	50.1078	50.3010	50.3109	1
	5	50.2546	50.0465	50.3725	50.2400	49.8584	50.1838	50.2688	2
	6	50.2910	50.2846	50.1656	50.1838	50.2546	50.1838	50.2993	1
	7	50.2688	50.0465	50.2993	49.9889	50.2393	50.2028	50.3238	1
	8	50.2688	50.2546	50.3400	50.3400	50.3238	50.2993	50.3400	1
Test 2	4	53.2509	53.6852	52.8906	52.6738	53.1883	53.4994	55.0746	1
	5	53.8415	53.4257	52.8211	54.0195	53.9520	53.0913	54.1916	1
	6	53.5883	54.3038	53.4994	53.3906	52.9730	53.1549	54.8516	1
	7	53.7337	54.0195	53.3553	54.0959	54.1916	53.1549	54.6424	1
	8	54.0959	53.9520	53.8988	52.8443	54.6424	52.9175	54.4554	2
Test 3	4	52.5759	53.0410	57.9629	54.0800	60.4387	56.2154	61.7181	1
	5	58.1025	61.9955	60.7466	61.7921	55.6256	64.5360	62.2837	2
	6	63.5360	61.4155	61.8584	63.9955	63.0681	62.4628	64.1239	1
	7	63.8109	63.9835	63.5676	61.4832	62.4628	62.9716	63.9835	1
	8	62.0349	63.6832	62.0349	64.3305	63.2450	63.6832	64.9955	1
Test 4	4	50.7395	51.1804	50.9108	51.2395	51.5061	51.0071	51.6027	1
	5	50.7715	51.2697	50.9807	51.4779	51.4481	50.9807	51.9066	1
	6	51.2087	51.5362	51.5680	50.9540	51.0893	50.9807	51.6027	1
	7	51.5680	51.7787	51.0332	51.5061	51.3279	51.4779	52.3334	1
	8	51.6027	51.3022	51.9066	51.8435	51.6770	50.9316	51.9874	1
Test 5	4	66.3989	66.3226	66.1569	66.2315	65.8829	63.6053	68.5931	1
	5	67.0276	66.6360	67.8621	67.7120	68.0244	67.7120	68.0276	1
	6	66.0897	67.0276	66.1569	68.0244	67.8621	66.0897	68.2168	1
	7	66.8126	67.8621	66.7116	68.0244	66.3226	68.0244	68.1207	1
	8	67.2603	67.4012	67.0244	67.7120	66.8126	67.7120	67.5643	2
Test 6	4	54.2026	54.4273	55.3578	53.7549	53.8915	53.5513	54.8571	2
	5	54.1463	54.5804	54.4870	55.1201	54.2885	54.4554	54.7820	2
	6	55.4150	54.4554	54.7820	55.3061	55.8798	55.9454	56.2736	1
	7	55.2543	54.8194	54.4554	54.5804	55.0305	54.6399	56.5408	1
	8	54.7820	54.1180	54.9437	54.5804	55.0305	54.4012	55.0305	1
Test 7	4	49.6997	50.0000	50.1370	49.9625	50.1052	50.0511	50.1844	1
	5	50.1844	49.9758	49.6021	50.0783	50.0909	49.9758	50.2244	1
	6	49.8357	50.1582	50.1370	50.1582	50.6934	50.1370	50.1844	1
	7	49.9879	50.0129	50.0646	50.1216	49.9758	49.9367	50.1582	1
	8	50.1052	50.0646	49.9004	50.1582	50.4270	50.2946	50.1844	1
Test 8	4	61.8856	64.1345	68.2224	65.1150	71.2205	65.5497	73.2257	1
	5	73.2257	65.1150	64.9807	66.4002	65.3866	72.6418	66.8555	3
	6	63.7686	67.2286	65.1150	64.1345	72.9845	68.2224	73.1019	1
	7	68.2224	65.5497	72.8406	66.6121	66.0254	67.2286	73.1019	1
	8	64.9807	65.5497	68.2224	65.5497	64.9807	65.1150	68.2224	1
Test 9	4	50.9997	50.7691	50.5773	50.8428	50.8303	50.9223	51.5932	1
	5	50.9691	50.7520	50.7422	50.7691	50.8428	50.7422	51.1273	1
	6	50.8214	50.6535	50.7884	50.7520	50.8639	50.7884	50.9436	1

Table 7 (continued)

Images	k	PSNR values							
		BA	DOA	FPA	MFO	SCA	GJO	SCGJO	Rank
	7	51.1920	51.6705	51.1273	50.8303	50.9072	50.7986	51.9473	1
	8	50.8639	51.2601	50.8639	51.5098	50.8214	50.7884	51.9850	1
Test 10	4	53.5340	57.2359	56.3238	57.8952	55.8911	57.5332	58.0853	1
	5	55.3489	57.4320	56.6876	55.4257	57.2359	56.8693	57.8693	1
	6	56.5239	56.8853	56.3238	56.8055	56.2359	56.6876	56.9390	1
	7	57.4320	58.0558	56.7466	57.6406	56.6876	57.4320	57.6853	2
	8	57.2376	57.6406	56.3238	57.2376	56.0162	56.7466	57.2584	2
Test 11	4	51.0604	51.1369	54.4533	51.0946	51.0840	53.4495	55.0750	1
	5	54.2209	56.2064	53.5446	51.0681	55.6387	56.4738	56.4738	1
	6	56.7982	56.0074	56.4237	56.3644	56.1308	56.2064	56.7982	1
	7	56.3090	55.7168	55.2583	56.9724	55.7978	56.4738	56.5064	1
	8	55.9281	54.0374	55.7578	56.7300	56.1095	56.1566	56.4237	2
Test 12	4	70.2348	71.1983	72.9060	74.1087	70.5346	69.7111	75.7489	1
	5	74.1087	74.1087	74.9418	68.9826	72.5005	71.6067	75.7489	1
	6	73.4709	71.9483	74.9418	73.4709	73.4709	77.0875	77.0875	1
	7	73.4709	71.9483	75.7489	75.7489	70.8565	74.1087	78.8642	1
	8	74.1087	74.9418	74.9418	73.4709	71.6067	74.9418	77.0875	1

The SSIM of each algorithm based on Kapur's entropy method is shown in Table 8. By establishing the structural information to retain the scene object's structure irrespective of brightness and contrast, the SSIM assesses the similarity between the source image and the segmented image. Distortion is characterized by the combination of three distinct elements: brightness, contrast, and structure. The brightness is measured by the pixel mean, contrast is calculated by the standard deviation, and the structural similarity is determined by the covariance. The SSIM value ranges erratically from 0 to 1. A higher SSIM value illustrates that the segmentation quality is greater and the calculation precision is better, and the disparity between the source image and the segmented image is relatively minimal. When the SSIM value is equal to 1, both images are exactly equivalent. The SSIM value rises when the threshold level is raised, the segmented image not only substantially diminished distortion degree but also is infinitely close to the source image. To confirm the overall segmentation ability of the SCGJO, the SSIM value is employed to arrive at the ranking, the SCGJO has a higher ranking and a superior SSIM value, which illustrates that the SCGJO has excellent stability and durability to accomplish the segmentation quality. There are 60 SSIM values for each algorithm, and the 55 SSIM values of the SCGJO are the best compared to the BA, DOA, FPA, MFO, SCA and GJO. The segmentation effect of the SCGJO is superior to those of other algorithms, and the disparity is remarkable. The experimental results demonstrate that the SCGJO not only exhibits extensive exploration and exploitation to avoid search stagnation and obtain the best SSIM values but also has good stability and similarity to accomplish greater computational precision and superior segmentation quality.

Table 8 The SSIM of each algorithm

Images	k	SSIM values							
		BA	DOA	FPA	MFO	SCA	GJO	SCGJO	Rank
Test 1	4	0.8362	0.8314	0.8049	0.8108	0.8346	0.8267	0.8375	1
	5	0.8615	0.8471	0.8377	0.8428	0.8297	0.8562	0.8642	1
	6	0.8477	0.8627	0.8707	0.8655	0.8690	0.8631	0.8768	1
	7	0.8696	0.8544	0.8700	0.8543	0.8741	0.8735	0.8752	1
	8	0.8579	0.8796	0.8671	0.8668	0.8782	0.8730	0.8797	1
Test 2	4	0.6642	0.6795	0.6362	0.6123	0.6469	0.6847	0.7179	1
	5	0.7113	0.6845	0.6021	0.7208	0.6784	0.6656	0.7315	1
	6	0.6724	0.7430	0.6905	0.6827	0.6482	0.6650	0.7596	1
	7	0.7017	0.7495	0.6708	0.7490	0.7469	0.6785	0.7786	1
	8	0.7068	0.7324	0.7133	0.6547	0.7581	0.6251	0.7798	1
Test 3	4	0.5962	0.6277	0.6511	0.6719	0.8313	0.7432	0.8398	1
	5	0.7867	0.8593	0.8468	0.8694	0.7263	0.8566	0.8708	1
	6	0.8450	0.8601	0.8637	0.8629	0.8715	0.8858	0.8898	1
	7	0.8815	0.8945	0.8916	0.8850	0.8817	0.8947	0.8958	1
	8	0.8931	0.8991	0.8940	0.8708	0.9029	0.8984	0.9097	1
Test 4	4	0.5370	0.5951	0.5744	0.6078	0.6205	0.5774	0.6212	1
	5	0.5192	0.6310	0.5912	0.6412	0.6416	0.5874	0.6484	1
	6	0.6341	0.6441	0.6512	0.5723	0.6103	0.5896	0.6626	1
	7	0.6784	0.6840	0.5799	0.6658	0.6406	0.6525	0.6890	1
	8	0.6858	0.6546	0.6923	0.6978	0.6788	0.5825	0.7092	1
Test 5	4	0.8781	0.8947	0.8775	0.9054	0.8878	0.8992	0.9088	1
	5	0.9076	0.9037	0.8846	0.8755	0.8957	0.9106	0.9117	1
	6	0.9127	0.8919	0.9256	0.9064	0.8802	0.9219	0.9321	1
	7	0.9392	0.9063	0.9365	0.8998	0.9121	0.9133	0.9377	2
	8	0.9361	0.9500	0.9355	0.9482	0.9372	0.9492	0.9524	1
Test 6	4	0.7614	0.7664	0.7453	0.7055	0.7332	0.7234	0.7742	1
	5	0.7802	0.7539	0.7908	0.7877	0.7767	0.7879	0.8028	1
	6	0.8435	0.8161	0.8172	0.8468	0.8256	0.8052	0.8566	1
	7	0.8555	0.8090	0.8148	0.8029	0.8172	0.7966	0.8249	2
	8	0.8483	0.8128	0.8628	0.8420	0.8485	0.8065	0.8597	2
Test 7	4	0.2641	0.2929	0.2990	0.2921	0.2348	0.2928	0.3054	1
	5	0.2610	0.3054	0.2662	0.3211	0.2612	0.2911	0.3222	1
	6	0.2971	0.3311	0.3275	0.3329	0.2946	0.3377	0.3569	1
	7	0.3295	0.3290	0.3336	0.3289	0.2636	0.3097	0.3520	1
	8	0.3266	0.3445	0.3251	0.3496	0.2359	0.3709	0.3735	1
Test 8	4	0.9018	0.9035	0.9058	0.9011	0.9079	0.9015	0.9098	1
	5	0.9113	0.9117	0.9094	0.9099	0.9034	0.9127	0.9147	1
	6	0.9318	0.9248	0.9191	0.9284	0.9301	0.9284	0.9369	1
	7	0.9277	0.9321	0.9355	0.9237	0.9317	0.9334	0.9438	1
	8	0.9393	0.9452	0.9432	0.9398	0.9399	0.9435	0.9452	1
Test 9	4	0.6963	0.6773	0.6421	0.6797	0.6673	0.6922	0.7009	1
	5	0.7042	0.6824	0.6777	0.6814	0.6683	0.6757	0.7126	1
	6	0.6891	0.6578	0.6865	0.6809	0.6955	0.6614	0.6937	2

Table 8 (continued)

Images	k	SSIM values							
		BA	DOA	FPA	MFO	SCA	GJO	SCGJO	Rank
	7	0.7175	0.7615	0.7101	0.6859	0.7049	0.6897	0.7589	2
	8	0.7042	0.7209	0.6794	0.7621	0.6729	0.6928	0.7831	1
Test 10	4	0.6958	0.7989	0.8488	0.8271	0.8185	0.8235	0.8559	1
	5	0.8190	0.8733	0.8595	0.8142	0.8246	0.8740	0.8868	1
	6	0.8749	0.8795	0.8826	0.8975	0.8767	0.8579	0.9004	1
	7	0.9045	0.8955	0.9019	0.9076	0.9079	0.9167	0.9192	1
	8	0.9199	0.9118	0.8968	0.9175	0.8608	0.9052	0.9258	1
Test 11	4	0.4973	0.5065	0.7252	0.5010	0.5052	0.6630	0.7643	1
	5	0.7017	0.7011	0.6660	0.5043	0.7902	0.7915	0.7975	1
	6	0.8137	0.8181	0.7802	0.8212	0.7805	0.7914	0.8205	1
	7	0.8289	0.8124	0.7933	0.8035	0.8161	0.8030	0.8355	1
	8	0.8378	0.7033	0.8213	0.8106	0.8399	0.8355	0.8504	1
Test 12	4	0.8106	0.8196	0.8186	0.8357	0.8197	0.8305	0.8358	1
	5	0.8302	0.8594	0.8669	0.8508	0.8346	0.8404	0.8678	1
	6	0.8787	0.8903	0.8779	0.8978	0.8834	0.8940	0.8980	1
	7	0.9007	0.9110	0.8499	0.8869	0.9122	0.9002	0.9149	1
	8	0.9158	0.9100	0.9101	0.9154	0.9259	0.9139	0.9264	1

The *p value* of the Wilcoxon rank-sum is shown in Table 9. The Wilcoxon's rank-sum test is employed to confirm if there is a substantial disparity between the two groups of data. $p < 0.05$ illustrates that there is a substantial disparity. $p \geq 0.05$ illustrates that there is no substantial disparity. The experimental results demonstrate that the disparity between the SCGJO and other algorithms is substantial, and the data is actual and reliable, not obtained by accident.

The segmented images of the SCGJO and other evolutionary algorithms under different threshold levels are shown in Figs. 4, 5, 6, 7, 8, 9, 10, 11, 12, 13, 14 and 15. For image segmentation, the intention is to actualize the accurate threshold values and the maximum objective values. As the threshold level rises, the optimization ability and segmentation performance of these algorithms will dramatically enhance, which illustrates that the SCGJO not only utilizes the collaborative foraging mechanism to balance exploration and exploitation but also has sufficient predictability and reliability to mitigate search stagnation and determine the high-quality segmented image with more valuable information. The SCGJO and other algorithms are employed to address the image segmentation, the segmentation quality and the overall optimal value of the SCGJO are superior to those of BA, DOA, FPA, MFO, SCA, and GJO. The SCGJO has superior fitness values and threshold values when compared to other algorithms, which illustrates that the SCGJO delivers complementary benefits to mitigate premature convergence and determine a better segmentation effect and higher segmentation accuracy. The PSNR values and the SSIM values of the SCGJO are superior to those of BA, DOA, FPA, MFO, SCA, and GJO which illustrates

Table 9 The *p value* of Wilcoxon rank-sum

Images	k	Wilcoxon rank-sum					
		BA	DOA	FPA	MFO	SCA	GJO
Test 1	4	4.91E-03	3.70E-03	4.17E-02	5.31E-03	2.36E-02	3.87E-02
	5	1.32E-03	7.50E-04	3.39E-02	1.63E-02	7.97E-04	1.66E-02
	6	4.48E-08	1.04E-02	9.11E-03	3.46E-03	1.08E-02	2.44E-02
	7	1.99E-08	3.57E-04	1.39E-02	4.75E-02	3.45E-02	6.73E-02
	8	2.46E-06	4.08E-02	4.14E-02	1.16E-02	8.00E-04	8.28E-04
Test 2	4	4.07E-03	1.01E-02	4.01E-02	6.34E-03	4.62E-02	3.52E-03
	5	3.79E-05	5.26E-04	3.34E-02	4.67E-02	5.25E-03	7.43E-04
	6	1.27E-09	8.69E-07	2.19E-02	6.75E-04	3.70E-02	6.02E-02
	7	2.43E-10	3.98E-02	5.92E-03	3.74E-03	2.06E-02	4.50E-02
	8	2.39E-10	6.04E-03	7.33E-03	3.81E-03	1.56E-02	5.30E-02
Test 3	4	1.26E-02	3.99E-02	5.89E-03	6.69E-03	2.90E-02	4.95E-02
	5	1.29E-05	3.29E-02	7.39E-03	3.36E-02	5.78E-03	6.30E-02
	6	5.56E-07	8.87E-03	8.41E-04	2.02E-02	4.36E-02	2.63E-02
	7	9.98E-09	5.36E-03	2.93E-02	4.66E-05	2.72E-02	1.27E-02
	8	2.36E-07	1.38E-02	1.28E-02	2.59E-02	5.18E-02	2.47E-02
Test 4	4	9.40E-03	6.88E-02	3.04E-02	3.48E-02	6.10E-03	9.41E-04
	5	2.15E-04	9.70E-04	6.19E-02	5.75E-03	9.05E-04	1.48E-02
	6	5.44E-07	4.30E-02	8.18E-03	6.36E-02	4.31E-04	8.99E-03
	7	1.04E-09	7.99E-03	8.88E-03	1.09E-02	2.88E-02	2.15E-02
	8	6.86E-08	7.71E-03	9.59E-03	1.37E-02	5.64E-02	8.18E-02
Test 5	4	2.74E-03	5.07E-05	5.30E-02	5.13E-03	9.96E-04	1.08E-02
	5	1.98E-06	8.72E-03	3.27E-02	5.03E-03	1.04E-02	5.37E-03
	6	4.47E-10	2.59E-02	6.89E-03	5.02E-03	4.49E-02	2.91E-02
	7	6.07E-09	2.08E-02	4.91E-02	7.64E-04	9.64E-03	2.37E-02
	8	1.42E-10	8.14E-01	6.00E-02	9.95E-04	1.65E-02	2.11E-02
Test 6	4	1.21E-02	9.59E-03	1.98E-02	1.01E-02	4.11E-02	8.13E-03
	5	3.97E-05	9.70E-03	3.98E-02	6.13E-03	7.17E-02	8.24E-04
	6	1.60E-08	9.35E-04	9.41E-03	4.19E-03	3.32E-02	8.94E-04
	7	2.11E-10	3.58E-02	4.89E-02	7.53E-04	1.69E-02	3.16E-02
	8	1.15E-09	1.79E-02	8.14E-03	1.43E-03	4.51E-02	4.84E-02
Test 7	4	2.96E-11	5.06E-06	2.99E-11	1.18E-08	2.38E-04	1.72E-07
	5	1.19E-10	2.01E-08	3.02E-11	6.59E-09	6.67E-03	3.02E-11
	6	4.49E-11	4.62E-10	3.02E-11	5.31E-10	1.49E-04	3.02E-11
	7	2.92E-11	3.01E-11	3.02E-11	2.56E-11	2.57E-07	3.02E-11
	8	2.52E-11	3.01E-11	3.02E-11	2.83E-11	1.70E-08	3.02E-11
Test 8	4	1.18E-02	2.38E-02	3.47E-02	7.94E-04	4.15E-03	2.10E-02
	5	2.32E-05	9.35E-03	4.37E-02	7.45E-04	5.28E-02	2.95E-02
	6	4.98E-10	2.60E-02	7.16E-03	1.91E-03	1.43E-02	9.35E-04
	7	3.74E-08	3.56E-02	4.40E-02	7.77E-04	4.82E-03	4.71E-02
	8	9.36E-11	9.64E-03	4.10E-02	7.44E-04	7.73E-04	7.17E-03
Test 9	4	1.33E-02	7.70E-02	3.78E-02	3.65E-02	9.65E-04	4.15E-02
	5	1.28E-05	2.52E-02	5.47E-02	1.12E-03	1.47E-02	5.13E-02
	6	1.52E-04	6.48E-04	5.87E-02	6.61E-03	1.66E-02	1.35E-02

Table 9 (continued)

Images	k	Wilcoxon rank-sum					
		BA	DOA	FPA	MFO	SCA	GJO
	7	1.34E-06	2.71E-02	9.82E-03	1.04E-03	1.65E-02	4.27E-02
	8	8.06E-09	8.04E-03	7.10E-03	1.08E-03	6.77E-03	7.83E-04
Test 10	4	9.28E-04	1.80E-02	4.63E-03	2.86E-02	2.57E-02	8.18E-04
	5	7.91E-06	4.91E-02	5.47E-03	7.37E-03	1.43E-02	1.07E-02
	6	9.45E-08	8.17E-03	6.09E-03	1.28E-03	6.50E-03	2.38E-02
	7	6.70E-09	2.50E-02	7.90E-03	8.13E-04	1.73E-03	3.03E-02
	8	2.06E-10	9.34E-03	1.14E-02	7.92E-04	1.69E-02	2.69E-02
Test 11	4	2.70E-02	7.83E-02	1.16E-02	8.45E-04	7.99E-04	9.35E-03
	5	4.80E-06	3.54E-03	2.16E-02	2.79E-02	2.87E-02	4.08E-02
	6	4.00E-09	7.09E-03	1.80E-02	1.07E-03	3.05E-03	6.65E-02
	7	5.93E-09	6.73E-03	5.88E-03	3.13E-02	2.49E-02	7.88E-03
	8	7.75E-10	5.72E-04	4.32E-02	9.66E-04	3.70E-02	4.86E-02
Test 12	4	1.15E-03	3.98E-02	8.53E-03	1.52E-02	1.91E-02	7.09E-02
	5	2.90E-02	2.13E-02	1.39E-02	9.22E-04	8.10E-04	2.03E-02
	6	4.19E-06	1.64E-02	1.93E-02	4.43E-02	1.88E-02	1.16E-02
	7	2.67E-09	1.18E-02	4.07E-02	5.66E-03	1.06E-03	5.95E-04
	8	8.06E-09	5.38E-02	1.81E-02	5.62E-03	9.51E-04	2.01E-02

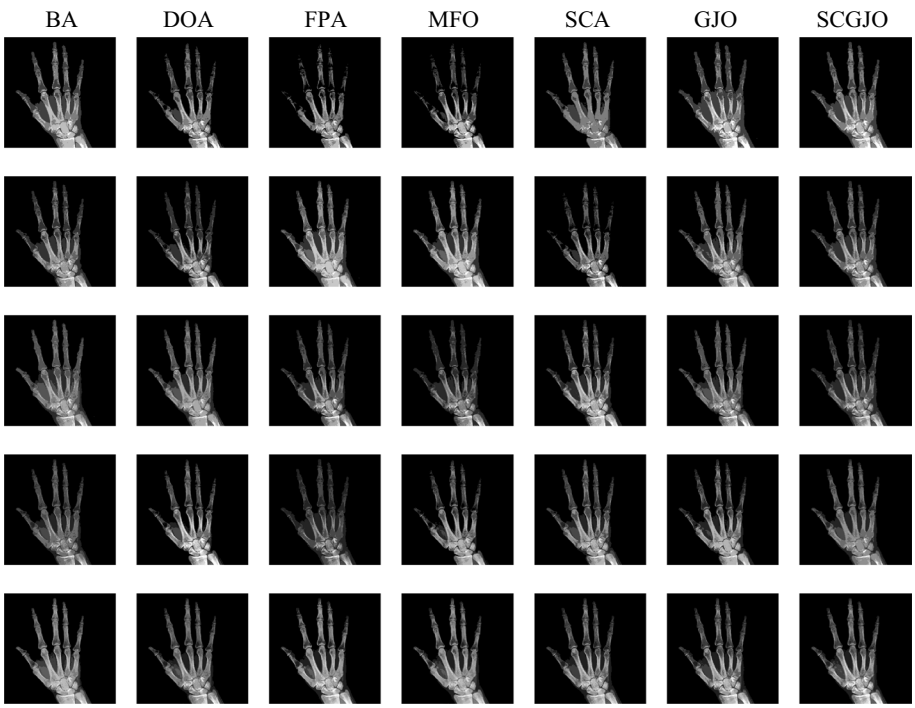

Fig. 4 Segmented images of Test 1

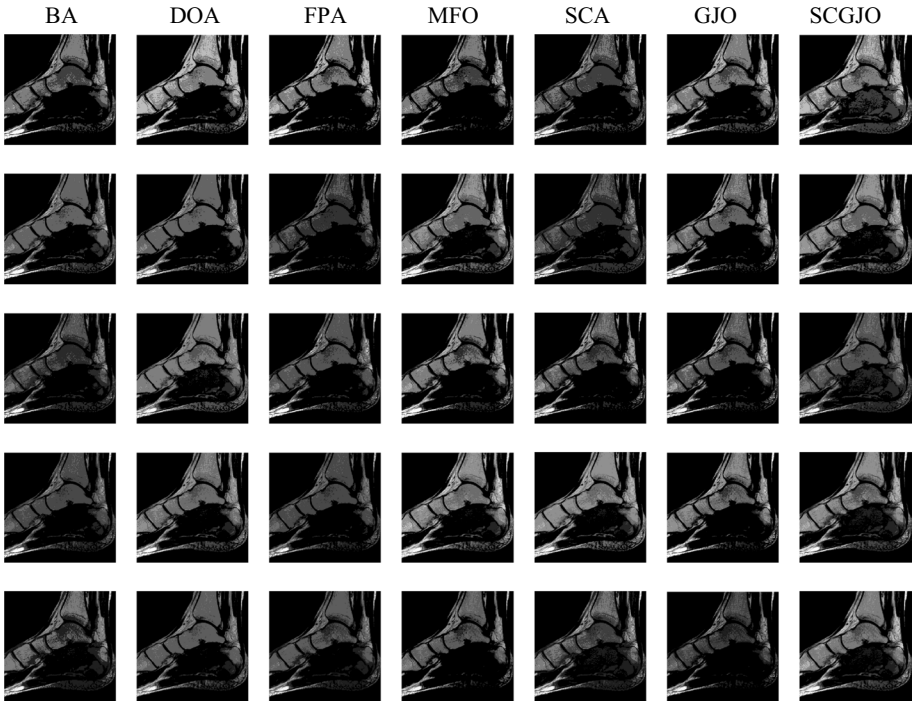

Fig. 5 Segmented images of Test 2

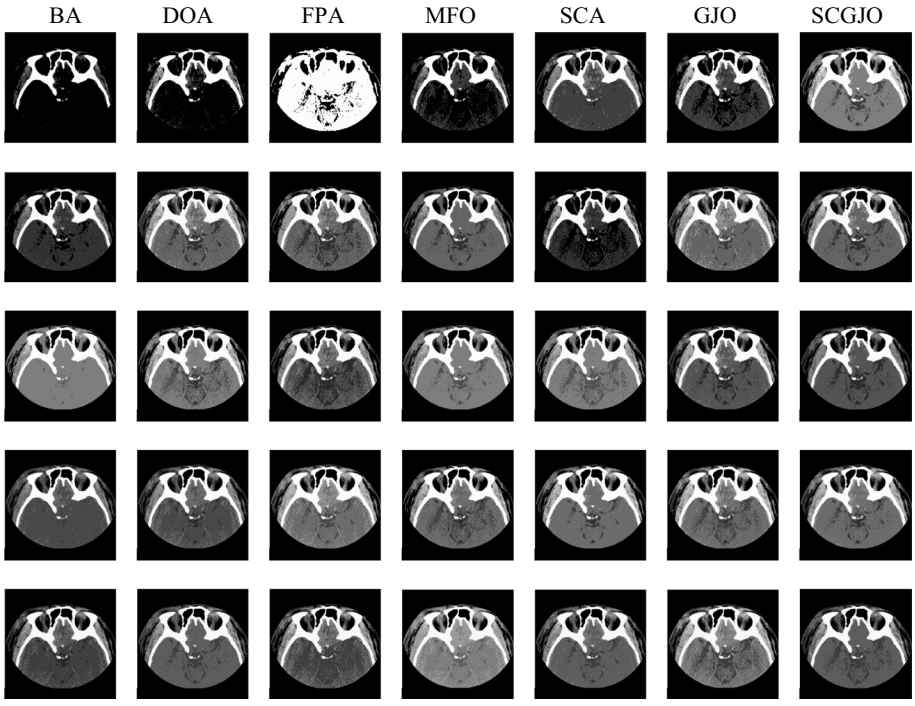

Fig. 6 Segmented images of Test 3

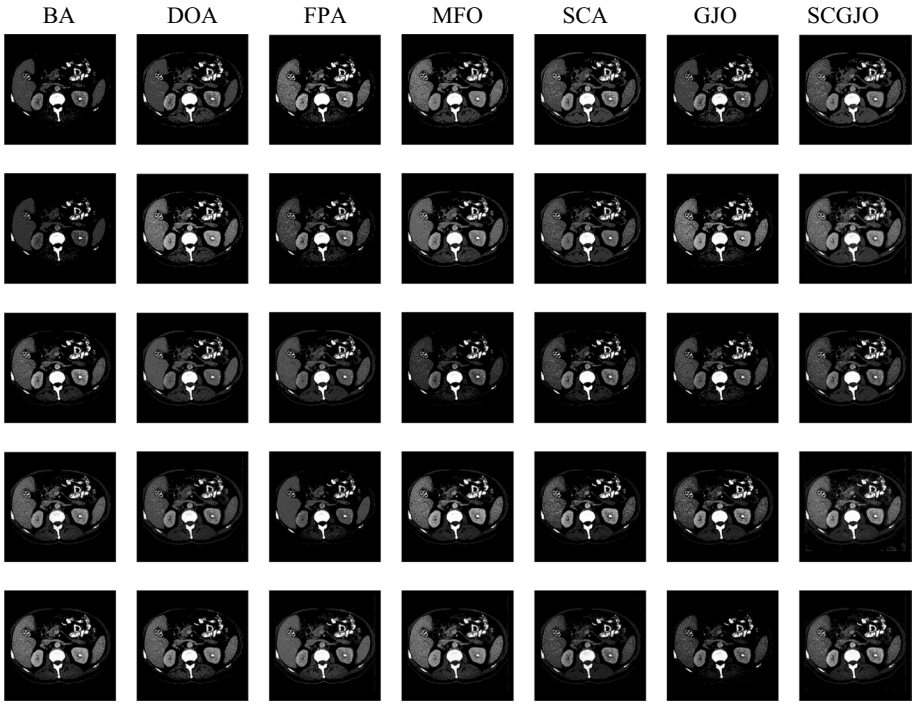

Fig. 7 Segmented images of Test 4

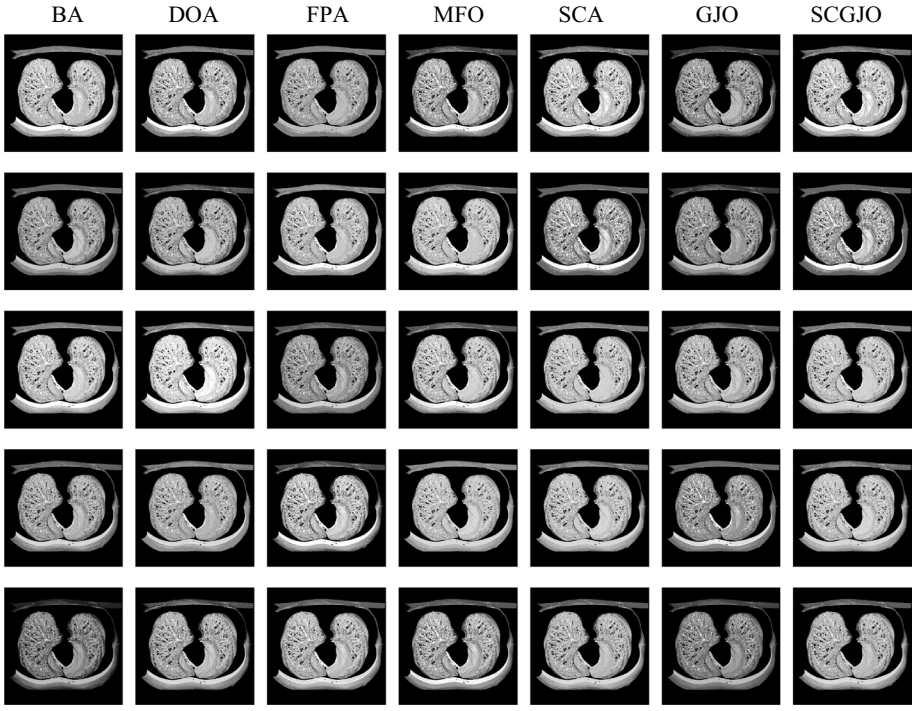

Fig. 8 Segmented images of Test 5

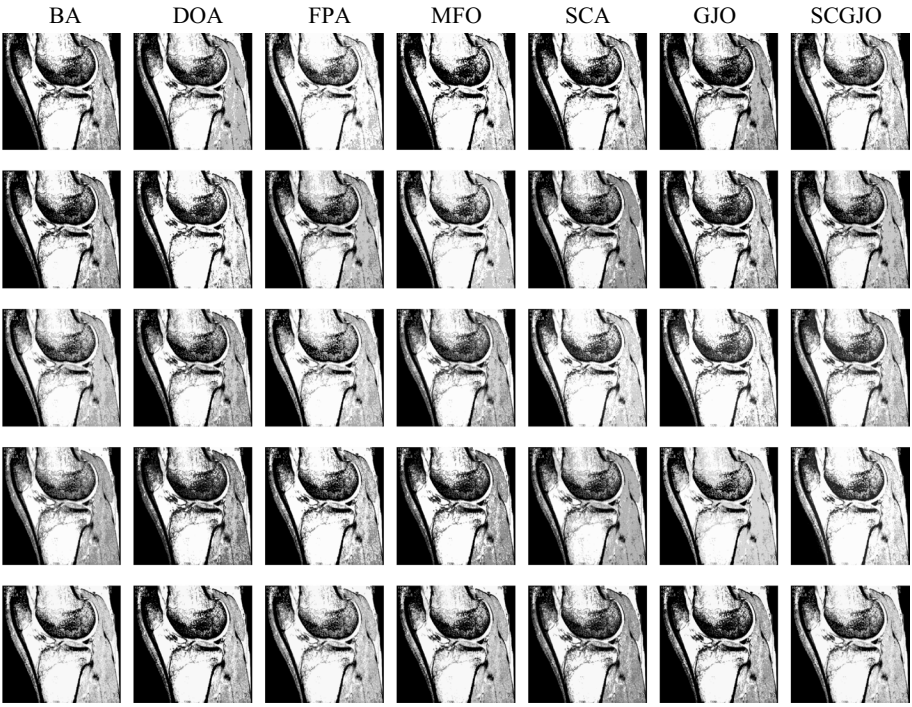

Fig. 9 Segmented images of Test 6

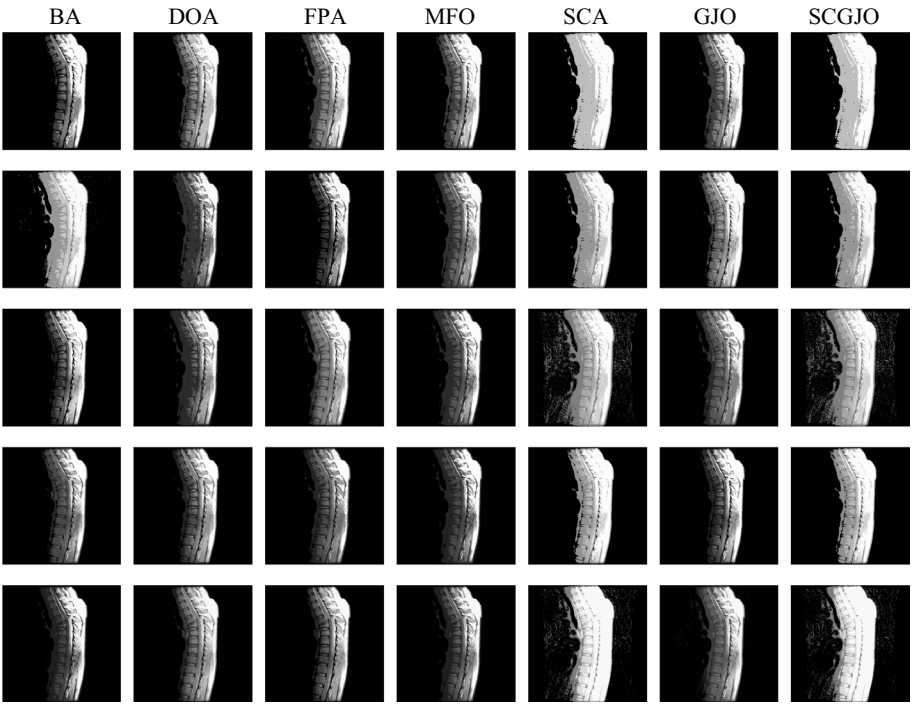

Fig. 10 Segmented images of Test 7

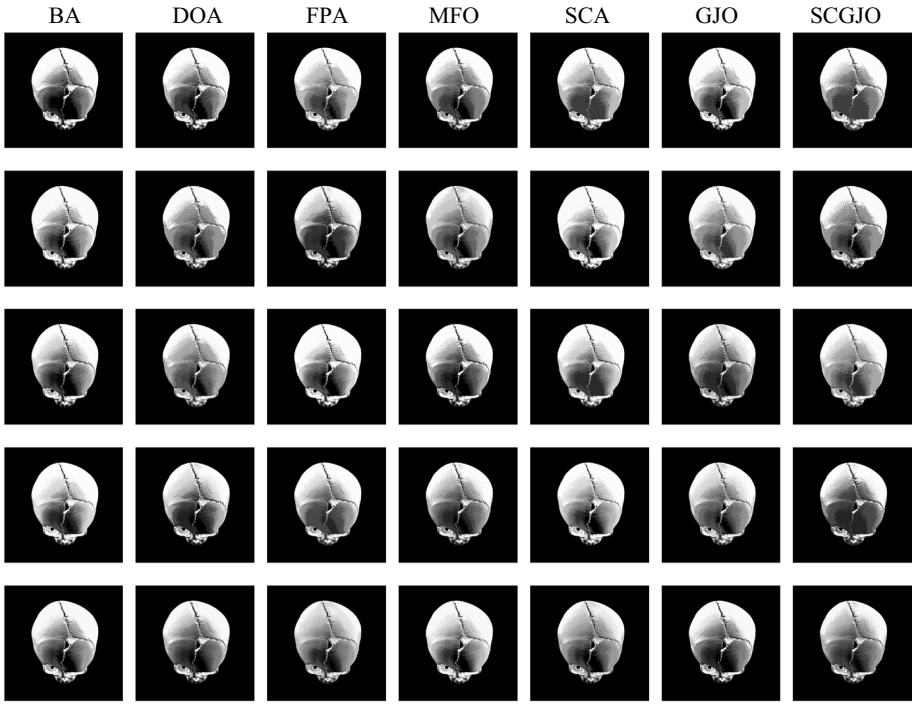

Fig. 11 Segmented images of Test 8

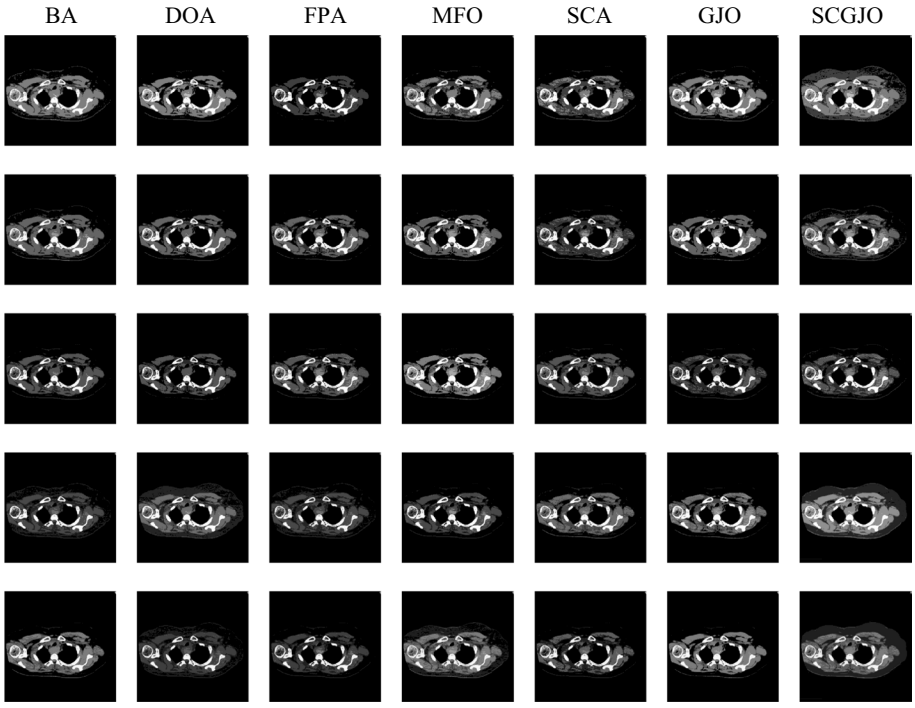

Fig. 12 Segmented images of Test 9

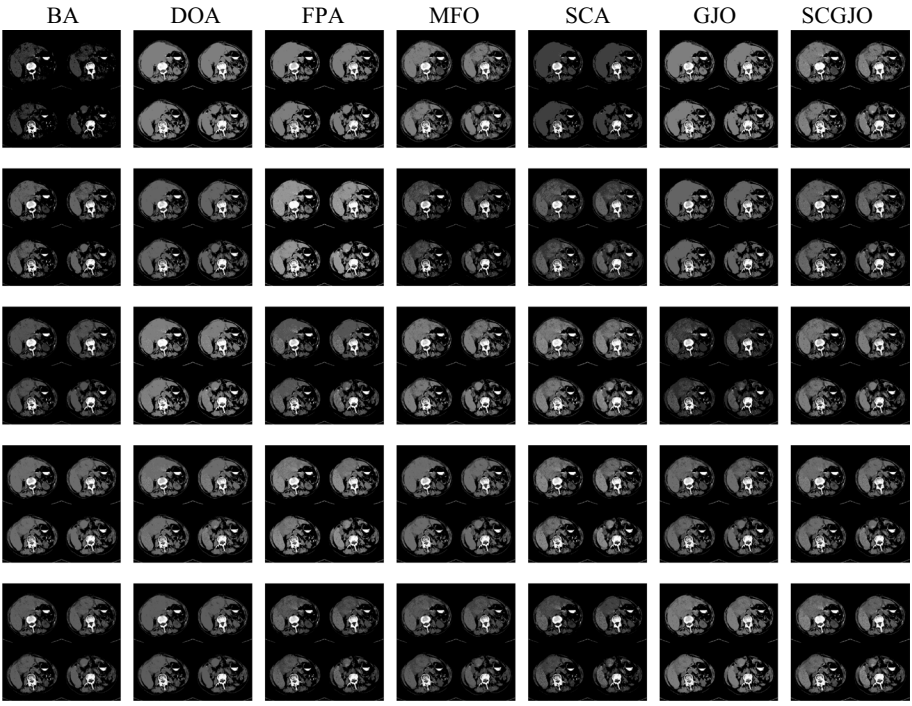

Fig. 13 Segmented images of Test 10

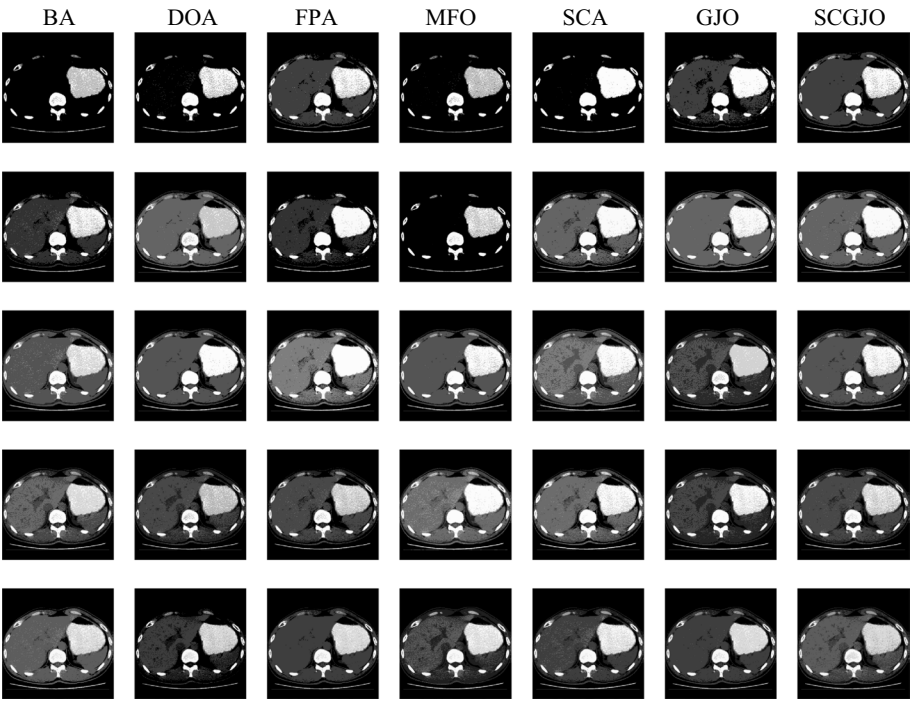

Fig. 14 Segmented images of Test 11

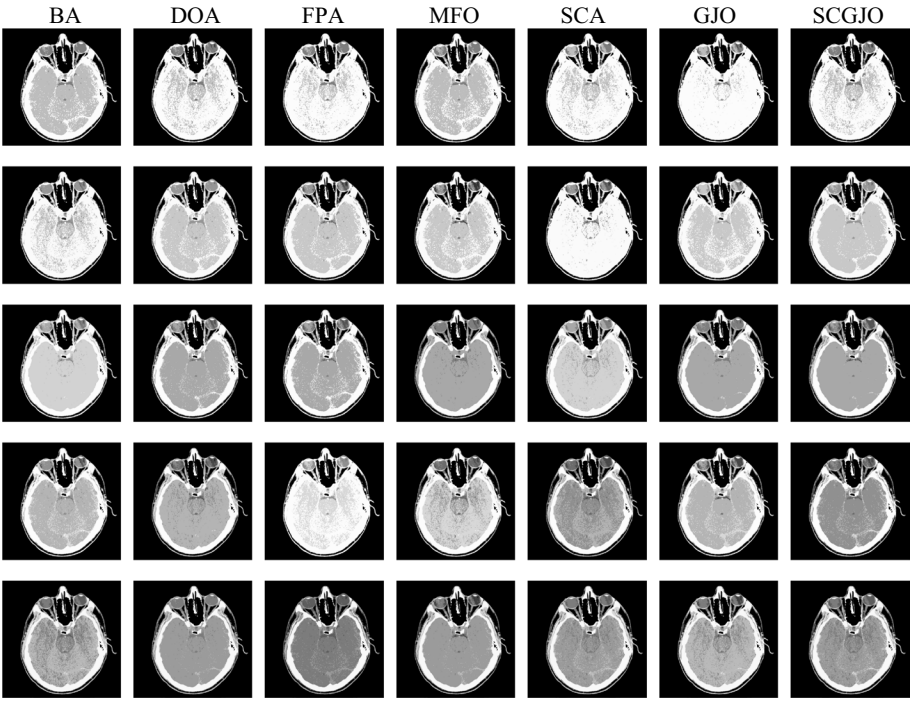

Fig. 15 Segmented images of Test 12

that the SCGJO not only integrates exploration and exploitation to promote the complementary benefits and mitigates search stagnation but also has fantastic stability and reliability to determine the better segmented images with less distortion degree and higher similarity. The SCGJO incorporates the advantages of GJO and SCA, which requires more time to accomplish the image segmentation and determine greater computational accuracy. The Wilcoxon rank-sum is employed to confirm if there is a substantial disparity between the two groups of data, the results demonstrate that the disparity between the SCGJO and other algorithms is noticeable. The experimental results demonstrate that the SCGJO exhibits exceptional robustness and stability to arrive at a faster convergence rate, higher calculation precision and greater segmentation quality.

Statistically, the SCGJO is based on the golden jackals' collaborative foraging behavior, which is utilized to address the image segmentation for the mentioned factors. First, the basic GJO has some disadvantages of premature convergence, search stagnation, inferior computation accuracy and sluggish convergence rate. The SCA is introduced into the GJO to strengthen both local and global search abilities, which is beneficial to achieve complementary advantages and determine the best solution. Second, SCGJO has the advantages of straightforward principles, accessible implementation, minimal parameters, strong stability and robustness. The SCGJO not only has strong superiority and stability to avoid search stagnation and achieves complementary benefits but also utilizes exploration and exploitation to determine a faster convergence rate, higher calculation precision and better segmentation quality. Third, the SCGJO imitates discovering prey, tracking and encircling prey, and trapping the prey to attain the global optimal value. The SCGJO has great robustness and resilience to address image segmentation and determine

a superior segmentation effect. The SCGJO employs the parameter $|E|$ to switch between exploration and exploitation and refresh the jackal's position. If $|E| \geq 1$, the SCGJO employs the discovering prey to promote the exploration and widen the search area. If $|E| < 1$, the SCGJO employs the tracking and enclosing prey, and trapping prey to promote exploitation and enhance convergence accuracy. To summarize, the SCGJO integrates exploration and exploitation to determine higher convergence accuracy and better segmentation quality, which is a reliable and consistent approach to address image segmentation.

7 Conclusions and future research

The SCA is added to the basic GJO to overcome the drawbacks of the basic GJO, premature convergence, sluggish convergence rate and inferior computation accuracy. In this paper, the SCGJO based on Kapur's entropy is presented to address the multilevel thresholding image segmentation, and the purpose is to maximize the fitness value and optimize the threshold values. The SCGJO utilizes the search mechanisms of discovering prey, tracking and encircling prey, and trapping prey to achieve efficient search and determine the best solution. A series of experiments are applied to demonstrate the overall segmentation quality of the SCGJO, the segmentation results are compared with those of the BA, DOA, FPA, MFO, SCA and GJO by achieving maximum the objective value of Kapur's entropy. As the threshold level increases, the SCGJO has certain superiority and stability to obtain better segmentation images with less distortion degree and higher similarity, and the disparity between the SCGJO and other algorithms is remarkable. The SCGJO not only has substantial resilience and durability to achieve complementary benefits and mitigate search stagnation but also employs exploration and exploitation to upgrade convergence accuracy and segmentation quality. The experimental results demonstrate that SCGJO is a persuasive and constructive approach, which has a faster convergence rate, higher calculation precision and better segmentation quality according to various evaluation indicators.

In future research, we will utilize the simulated annealing algorithm or genetic algorithm to address the image segmentation. The convergence rate and the calculation precision of the basic GJO will be enhanced by the addition of productive strategies, adoption of distinctive coding mechanisms, or combination with other algorithms. Different segmentation mechanisms will be employed to accomplish the color image segmentation with a high threshold level. We will consider the usage of more recent full-reference image quality assessment metrics where visual saliency is incorporated since the human visual system is not equally sensitive to all parts of the image.

Acknowledgments This work was partially funded by the Start-up Fee for Scientific Research of High-level Talents in 2022 under Grant No. 00701092336, and partly supported by the University Synergy Innovation Program of Anhui Province under Grant No. GXXT-2021-026, Smart Agriculture and Forestry and Smart Equipment Scientific Research and Innovation Team (Anhui Undergrowth Crop Intelligent Equipment Engineering Research Center) under Grant No. 2022AH010091, Scientific Research Project of University in Anhui Province under Grant Nos. 2022AH040241 and 2022AH051674.

Data availability The data set (s) supporting the conclusions of this article is (are) included within the article.

Declarations

Competing interests The authors declare that they have no known competing financial interests or personal relationships that could have appeared to influence the work reported in this paper.

CRediT authorship contribution statement **Jinzhong Zhang:** Conceptualization, Methodology, Software, Data curation, Formal analysis, Writing – original draft, Funding acquisition. **Gang Zhang:** Conceptualization, Methodology, Resources, Project administration, Funding acquisition. **Min Kong:** Conceptualization, Methodology, Writing – review & editing, Investigation. **Tan Zhang:** Validation, Writing – review & editing.

References

1. Aa A, Em B, Gvw C, Mb A (2018) Framework for reproducible objective video quality research with case study on PSNR implementations. Digit Signal Process 77:195–206
2. Abdel-Basset M, Chang V, Mohamed R (2021) A novel equilibrium optimization algorithm for multi-thresholding image segmentation problems. Neural Comput Applic 33:10685–10718
3. Abdel-Basset M, Mohamed R, AbdelAziz NM, Abouhawwash M (2022) HWOA: A hybrid whale optimization algorithm with a novel local minima avoidance method for multi-level thresholding color image segmentation. Expert Syst Appl 190:116145
4. Agrawal S, Panda R, Choudhury P, Abraham A (2022) Dominant color component and adaptive whale optimization algorithm for multilevel thresholding of color images. Knowl-Based Syst 240:108172
5. Al-Rahlawee ATH, Rahebi J (2021) Multilevel thresholding of images with improved Otsu thresholding by black widow optimization algorithm. Multimed Tools Appl 80:28217–28243
6. Anitha J, Pandian SIA, Agnes SA (2021) An efficient multilevel color image thresholding based on modified whale optimization algorithm. Expert Syst Appl 178:115003
7. Bairwa AK, Joshi S, Singh D (2021) Dingo optimizer: A nature-inspired metaheuristic approach for engineering problems Math Probl Eng 2021:
8. Bridge PD, Sawilowsky SS (1999) Increasing physicians' awareness of the impact of statistics on research outcomes: comparative power of the t-test and Wilcoxon rank-sum test in small samples applied research. J Clin Epidemiol 52:229–235
9. Chen K, Zhou F, Yin L et al (2018) A hybrid particle swarm optimizer with sine cosine acceleration coefficients. Inf Sci 422:218–241
10. Chopra N, Ansari MM (2022) Golden jackal optimization: A novel nature-inspired optimizer for engineering applications. Expert Syst Appl 198:116924
11. Chouksey M, Jha RK, Sharma R (2020) A fast technique for image segmentation based on two meta-heuristic algorithms. Multimed Tools Appl 79:19075–19127
12. Das G, Panda R, Samantaray L, Agrawal S (2022) A Novel Segmentation Error Minimization-Based Method for Multilevel Optimal Threshold Selection Using Opposition Equilibrium Optimizer. Int J Image Graph 2350021
13. Dinkar SK, Deep K, Mirjalili S, Thapliyal S (2021) Opposition-based Laplacian equilibrium optimizer with application in image segmentation using multilevel thresholding. Expert Syst Appl 174:114766
14. Duan L, Yang S, Zhang D (2021) Multilevel thresholding using an improved cuckoo search algorithm for image segmentation. J Supercomput 77:6734–6753
15. Gill HS, Khehra BS (2022) Apple image segmentation using teacher learner based optimization based minimum cross entropy thresholding. Multimed Tools Appl 81:11005–11026
16. Hayyolalam V, Kazem AAP (2020) Black widow optimization algorithm: a novel meta-heuristic approach for solving engineering optimization problems. Eng Appl Artif Intell 87:103249
17. Houssein EH, Emam MM, Ali AA (2021) An efficient multilevel thresholding segmentation method for thermography breast cancer imaging based on improved chimp optimization algorithm. Expert Syst Appl 185:115651
18. Houssein EH, Hussain K, Abualigah L et al (2021) An improved opposition-based marine predators algorithm for global optimization and multilevel thresholding image segmentation. Knowl-Based Syst 229:107348
19. Jiang Z, Zou F, Chen D, Kang J (2021) An improved teaching–learning-based optimization for multilevel thresholding image segmentation. Arab J Sci Eng 46:8371–8396
20. Kapur JN, Sahoo PK, Wong AK (1985) A new method for gray-level picture thresholding using the entropy of the histogram. Comput Vis Graph Image Proc 29:273–285

21. Kurmi Y, Chaurasia V (2021) Content-based image retrieval algorithm for nuclei segmentation in histopathology images. Multimed Tools Appl 80:3017–3037
22. Li X, Li X, Yang G (2022) A novelty harmony search algorithm of image segmentation for multilevel thresholding using learning experience and search space constraints. Multimed Tools Appl 1–21
23. Liu Q, Li N, Jia H et al (2022) Modified remora optimization algorithm for global optimization and multilevel thresholding image segmentation. Mathematics 10:1014
24. Liu X, Tian H, Wang Y et al (2022) Research on Image Segmentation Algorithm and Performance of Power Insulator Based on Adaptive Region Growing. J Electr Eng Technol:1–12
25. Ma G, Yue X (2022) An improved whale optimization algorithm based on multilevel threshold image segmentation using the Otsu method. Eng Appl Artif Intell 113:104960
26. Mirjalili S (2015) Moth-flame optimization algorithm: A novel nature-inspired heuristic paradigm. Knowl-Based Syst 89:228–249
27. Mirjalili S (2016) SCA: a sine cosine algorithm for solving optimization problems. Knowl-Based Syst 96:120–133
28. Mookiah S, Parasuraman K, Kumar Chandar S (2022) Color image segmentation based on improved sine cosine optimization algorithm. Soft Comput 1–11
29. Naik MK, Panda R, Samantaray L, Abraham A (2022) A novel threshold score based multiclass segmentation technique for brain magnetic resonance images using adaptive opposition slime mold algorithm. Int J Imaging Syst Technol
30. Patra DK, Si T, Mondal S, Mukherjee P (2022) Magnetic Resonance Image of Breast Segmentation by Multi-Level Thresholding Using Moth-Flame Optimization and Whale Optimization Algorithms. Pattern Recognit Image Anal 32:174–186
31. Sharma A, Chaturvedi R, Bhargava A (2022) A novel opposition based improved firefly algorithm for multilevel image segmentation. Multimed Tools Appl 81:15521–15544
32. Shi C, Lin Y (2022) Image quality assessment based on three features fusion in three fusion steps. Symmetry 14:773
33. Si T, Patra DK, Mondal S, Mukherjee P (2022) Breast DCE-MRI segmentation for lesion detection using Chimp Optimization Algorithm. Expert Syst Appl 117481
34. Singh S, Mittal N, Singh H (2020) A multilevel thresholding algorithm using LebTLBO for image segmentation. Neural Comput Applic 32:16681–16706
35. Subasree S, Sakthivel N, Balasaraswathi V, Tyagi AK (2022) Selection of Optimal Thresholds in Multi-Level Thresholding Using Multi-Objective Emperor Penguin Optimization for Precise Segmentation of Mammogram Images. J Circuits Syst Comput 31:2250131
36. Varga D (2022) Saliency-Guided Local Full-Reference Image Quality Assessment. Signals 3:483–496
37. Vijh S, Saraswat M, Kumar S (2022) Automatic multilevel image thresholding segmentation using hybrid bio-inspired algorithm and artificial neural network for histopathology images. Multimed Tools Appl 1–32
38. Wang Y, Song S (2022) An adaptive firefly algorithm for multilevel image thresholding based on minimum cross-entropy. J Supercomput 78:11580–11600
39. Wang Z, Bovik AC, Sheikh HR, Simoncelli EP (2004) Image quality assessment: from error visibility to structural similarity. IEEE Trans Image Process 13:600–612
40. Wang R, Zhou Y, Zhao C, Wu H (2015) A hybrid flower pollination algorithm based modified randomized location for multi-threshold medical image segmentation. Biomed Mater Eng 26:S1345–S1351
41. Wu D, Yuan C (2022) Threshold image segmentation based on improved sparrow search algorithm. Multimed Tools Appl 1–34
42. Yan Z, Zhang J, Tang J (2020) Modified water wave optimization algorithm for underwater multilevel thresholding image segmentation. Multimed Tools Appl 79:32415–32448
43. Yang X-S (2012) Flower pollination algorithm for global optimization. In: International conference on unconventional computing and natural computation. Springer, pp 240–249
44. Yang X-S (2013) Bat algorithm: literature review and applications. ArXiv Prepr ArXiv13083900
45. Zhang Y, Xie H, Sun J, Zhang H (2022) An efficient multi-level encryption scheme for stereoscopic medical images based on coupled chaotic system and Otsu threshold segmentation. Comput Biol Med 146:105542